H

HEAT FLOW MEASUREMENTS, CONTINENTAL

John H. Sass[1], Graeme Beardsmore[2,3]
[1]Great Lakes Geothermal Services, Port Huron, MI, USA
[2]Monash University, Melbourne, Australia
[3]Hot Dry Rocks Pty Ltd, Victoria, Australia

Definition

Continental heat flow is the flux density of heat being conducted to the surface of continents. It is expressed as mW m^{-2}. Heat flow is calculated as the product of temperature gradient (mK m^{-1} or °C per km – a scale appropriate to the dimensions of geological formations) and thermal conductivity (W m^{-1} K^{-1}).

Introduction

Terrestrial heat flow, Q, is estimated from the product of temperature gradient (Γ) and thermal conductivity (K), according to:

$$Q = K.\Gamma \tag{1}$$

In practice, Γ is derived from point measurements of temperature at two or more discrete depths. K can be determined in situ, but for routine determinations of heat flow, the most practical approach is to measure it on the surface, either in the field or in a laboratory.

Beardsmore and Cull (2001) reviewed the various options for applying equation 1. These usually involve combining the harmonic mean thermal conductivity and temperature gradient over discrete intervals of the temperature profiles. Where there is significant thermal conductivity stratification, the "Bullard plot" is a useful method for calculating average heat flow (see Figure 1). In this method, temperature is plotted against integrated thermal resistance, R, where $R = z/K$, z being the thickness of the interval with mean conductivity K. If heat flow is constant with depth, the relation is linear and the slope of the line is the heat flow.

Uncertainty is inherent in heat flow determinations:

- As thermal gradient estimates become more precise with increasing depth, thermal conductivity estimates become less precise.
- The average thermal gradient and the average thermal conductivity must be determined over the same depth interval for a precise determination of heat flow.
- Because it is rarely practical to measure thermal conductivity over an entire depth interval, assumptions must be made as to how representative the measured samples are of the entire depth interval.
- The thermal disturbance due to seasonal surface temperature cycles may extend to a depth of several tens of meters, so meaningful results can be obtained only at greater depths.
- The diffusion of step changes in surface temperature (e.g., from the retreat of glaciation) may affect heat flow measurements down to hundreds of meters or more.
- Continental heat flow measurements, especially when compared to measurements of heat flow beneath the oceans, are complicated by significant lateral and temporal variations in surface temperature.
- Surface heat flow on the continents is more likely than oceanic heat flow to be distorted by near-surface variations in geological structures and topography.

Derived heat flow values may vary depending on the depth and sampling strategy of the survey, so careful thought should precede the design of any survey aimed at quantifying regional terrestrial heat flow.

Temperature

The earliest measurements of temperature beneath the earth's surface were obtained from mines and tunnels. As exploratory drilling for petroleum and minerals

Harsh K. Gupta (ed.), *Encyclopedia of Solid Earth Geophysics*, DOI 10.1007/978-90-481-8702-7,

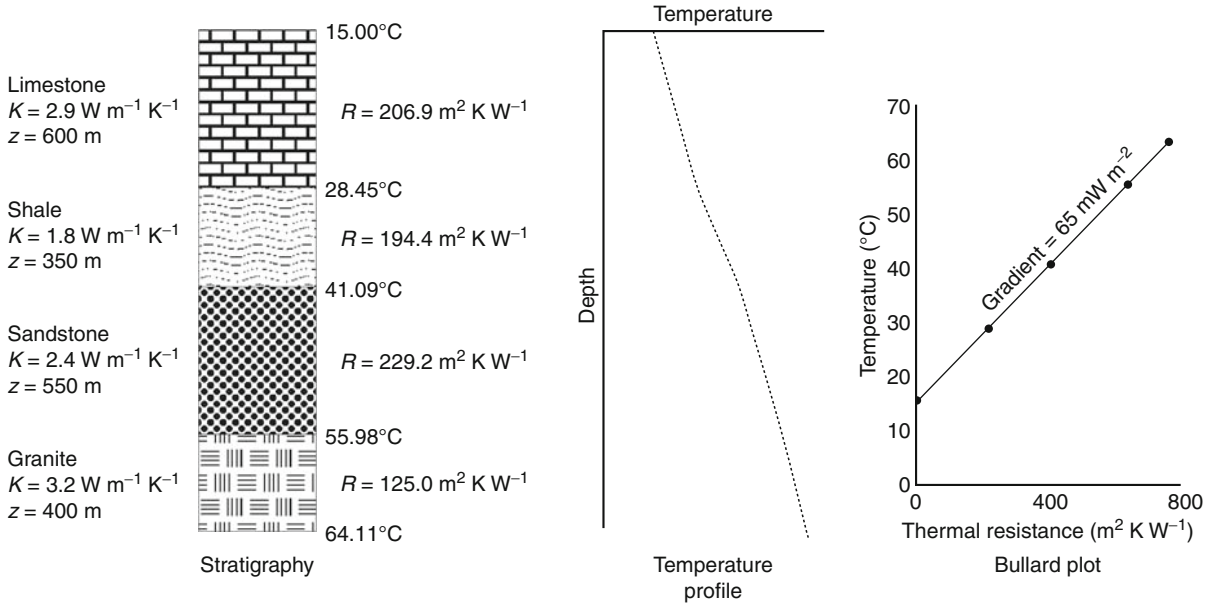

Heat Flow Measurements, Continental, Figure 1 A hypothetical rock sequence with thermal properties and unit thicknesses. The thermal resistance, *R*, of each unit is equal to its thickness, *z*, divided by its thermal conductivity, K. A temperature–depth profile through the sequence is nonlinear, but a Bullard plot of temperature versus integrated thermal resistance is linear with slope equal to the conductive heat flow. Heat flow in this example is 65 mW m^{-2}.

became widespread, temperature profiles obtained in boreholes became the most common means of determining temperature gradients within the earth. Almost exclusively, electronic thermometers deployed on a wire line are currently used to measure temperatures within the earth.

Temperature and depth measurements for heat flow determinations need to be precise and accurate. Best practice calls for a precision of ~0.001°C at ~1 m intervals over several hundred meters. Common transducers include the following types:

- Thermistors: A thermistor is a bead of sintered metallic oxide, commonly germanium. It has a large negative temperature coefficient of resistance (typically −4% per K), and is precise and accurate to 1 mK using simple, unsophisticated readout devices like off-balance Wheatstone bridges and 4½ digit multimeters (DMMs) (McGee and Thomas, 1988). Thermistor probes for use in "normal" geothermal environments usually have a resistance of between 3 and 100 KΩ at 25°C and provide useable readouts between about 0°C and 80°C, above which their temperature sensitivity drops off because of low resistance. Thermistors must be individually calibrated.
- Platinum Resistance Elements (RTDs): Platinum RTDs have a small, positive temperature coefficient of resistance and depending upon their construction and configuration, can operate successfully up to 500°C (see Tew and Strauss, 2001, for principles and standards). Millidegree accuracy can be obtained with RTDs if 6½ digit DMMs are employed as readouts. RTD probes for geothermal applications typically have a resistance of 1 or 2 KΩ at 20°C. One advantage over thermistors is the interchangeability of RTD probes within a batch without the need for individual calibration.
- Diodes: Effective temperature sensors can be constructed from ordinary semiconductor diodes. Such sensors have a linear voltage or current response with temperature, are of relatively small size, operate over a limited temperature range (typically −40°C to +120°C), are of low cost, and are quite accurate if individually calibrated. Diode temperature sensors tend to be less robust (electrically and physically) than other sensor types, which tends to rule them out of most logging applications. For stationary applications, however, commercial semiconductor sensors are available that provide an output signal as a voltage, a current, a resistance, or as digital data.
- Fiber Optics: Distributed fiber-optic measurement of temperature using the phenomenon of backscattering is possible using commercially available instruments with temperature resolution down to 0.01°C (Selker et al., 2006). Instantaneous records of temperature distribution along entire lengths of fiber-optic cable at intervals of ~1 m up to 30,000 m can be obtained at time intervals of fractions of a minute. Temperature resolution increases relative to the length of time over which each measurement is recorded. This technology holds great promise for repeated temperature profiles in a well recovering from drilling-associated thermal

transients, or for monitoring the thermal effects of pumping or injection in "Hot Dry Rock" applications. Förster et al. (1997) presented a comparison between fiber-optic and conventional temperature logs.

Temperature Tools include the following types:

- Four-conductor connection to the surface. This mode provides for accurate measurement of the resistance of the temperature transducer. It requires that the leakage resistance between conductors be effectively infinite, a specification that can be met by manufacturers of geophysical logging cables. Significant leakage between conductors is usually manifested as noise on the detector. The relatively high resistance of thermistors with respect to typical logging cable makes them the most suitable transducers for these tools.
- Down-hole oscillator with single-conductor transmission. Where suitable multi-conductor cables are not available, the resistance element can be incorporated into an oscillator circuit with temperature–frequency dependence, independent of leakage between conductors (Doig et al., 1961).
- "Memory tools." With or without onboard pressure gauges, memory tools are deployed on a wire line. They record down hole and store data in onboard memory. The data are downloaded and read on the surface (Suto et al., 2008).
- Fiber-optic cables: Henninges et al. (2005) described the deployment of fiber-optic cables for both synoptic temperature logs and long-term monitoring of temperature.

Thermal conductivity

There are two basic approaches for thermal conductivity measurement:

1. Steady State (divided bar)
2. Transient (point-, line- or plane- source)

The concept of the divided bar was originally introduced by Prof. C.H. Lees in the nineteenth century. The device is essentially a vertical "stack" within which the temperature drop across a standard substance is compared with that across a disc of unknown thermal conductivity. Early versions were introduced in the 1930s by Prof. E.C. Bullard at Cambridge and by Prof. Francis Birch at Harvard. These adaptations featured a constant heat source at the top of the "stack" and an isothermal sink at the base. Adoption of a constant temperature difference resulted in more rapid measurements (Beck, 1957). Substitution of Peltier devices for the constant temperature water baths usually used provides hitherto unattainable portability, economy and speed of measurement (Antriasian, 2010; Figure 2). In the late 1960s, the divided bar was adapted to the measurement of the thermal conductivity of rock fragments, by far the most common source of material (Sass et al., 1971).

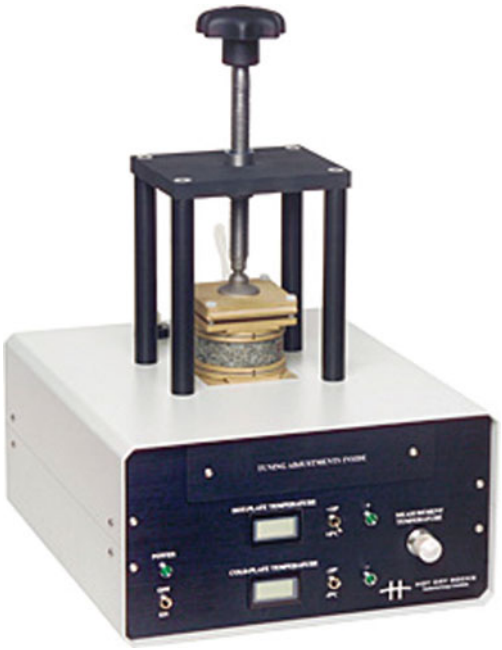

Heat Flow Measurements, Continental,
Figure 2 A commercial divided bar utilizing Peltier devices as heat source/sink. (Photo courtesy of Hot Dry Rocks Pty Ltd, Australia.)

Transient heat source methods can be applied in a permanent laboratory, in mobile field laboratories, or in certain circumstance within boreholes. In these techniques, the rock is heated, and the temperature-time curve of the heater element or a nearby point is analyzed to obtain the thermal conductivity. In general, higher conductivity rocks conduct heat away from the heater at a greater rate and suppress the increase in temperature.

Line- or cylindrical- source methods present difficulties in characterizing uniaxial (e.g., vertical) conductivity because they conduct heat radially, rather than linearly, away from the source. In homogenous sequences, conductivity is the same in all directions, but the values may be significantly different in heterogeneous sequences. Point source methods overcome this to some extent but require higher operating power and may initiate convection (thus negating the assumption of pure conduction).

J.C. Jaeger pioneered the concept of line- and cylindrical heat sources for the measurement of thermal conductivity. Early attempts at implementation of his models called for ingenuity in the use of analog recording devices of fairly low sensitivity. Line-source methods in common use include variations on the "needle probe" and half-space techniques; e.g., Showa Denko (Ito et al., 1977) and GeoForschungZentrum (GFZ) line-source units, see e.g., Pribnow and Sass (1995), which also has a description of the United States Geological Survey (USGS) divided bar apparatus. Both units are available commercially. K. Horai (1971) adapted the line-source

technique to measurements on fragments. The USGS versions of line-source techniques were described in detail by Sass et al. (1984).

Optical scanning

In the 1980s, Yuri Popov developed a rapid, nondestructive method for measuring the thermal conductivity of large numbers of rocks using an optical scanning technique. Flat and black-painted rock faces are aligned with a known standard material along a track. A device containing a laser heat source and an infrared radiometer temperature sensor moves at a constant speed across the surface of the samples. The radiometer measures the rise in temperature of the samples due to the applied laser pulse, and the temperature rise is then related back to the thermal conductivity of the rocks. This method was initially met with skepticism in many laboratories, but a three-way comparison among Popov's method, the USGS divided bar, and the GFZ line-source half-space apparatus resulted in remarkable agreement over a large range of thermal conductivity and a variety of crystalline rock types (Popov et al., 1999).

In situ thermal conductivity measurement in boreholes

The in situ measurement of thermal conductivity in vertical boreholes generally presents great experimental and logistical difficulties. In anisotropic rocks, it also measures conductivity in the wrong direction so that independent measurements of anisotropy on core are required to calculate vertical conductivity. Conductivity was measured in situ over a ~2 m interval of the KTB pilot core hole (Burkhardt et al., 1990) as a demonstration of the feasibility of the method.

During the boom in geothermal exploration in the mid- to late 1970s, the importance of determining heat flow, as well as temperature gradients became apparent. This was coupled with concerns over the security of exploration wells in competitive lease areas. To address these issues, the Geothermal Studies Project of the U.S. Geological Survey developed a method for determining temperature gradient, thermal conductivity, and thus, heat flow in situ over discrete intervals during the drilling process (Sass et al., 1981)

Details of the technology can be found in Sass et al. (1979) with the caveat that the electronics and computer hardware described in that reference have since been superseded.

More recently, Freifeld et al. (2008) have demonstrated thermal conductivity profiling of entire boreholes by coupling a down-hole line-source heating loop with a distributed fiber-optic temperature system.

Sampling

Thermal conductivity can rarely be practically measured over the full interval of interest. Certain sampling protocols must be devised and followed to estimate the conductivity over significant depth intervals. This may involve:

- Characterizing the conductivity of individual geological formations where these are largely homogenous
- Selecting samples from evenly spaced intervals as a "random" sampling strategy
- Measuring mixtures of chips from sequential depth intervals

Conductivity is temperature dependent and values measured in the laboratory should be corrected for in situ conditions especially for very deep wells, and in geothermal areas with high temperature gradients.

When no rock samples are available for measurement of thermal conductivity, estimates can be obtained from empirical relations between conductivity and well-log parameters or by choosing a "flux plate", a layer of more than a few meters thickness composed of a rock type whose conductivity has been characterized by measurements elsewhere. (See Blackwell and Steele, 1989 for a review of these methods.)

Summary

Heat flowing from the surface of the continents cannot be measured directly. It is calculated as the product of the temperature gradient (most often measured in boreholes) and the thermal conductivity of the formation within which the temperature gradient was measured. Thermal conductivity can be measured in situ, but by far the majority of measurements are made on rock samples from the borehole, or from nearby outcrops of the relevant formations.

Temperatures are usually measured by electronic transducers deployed on multi-conductor electrical cables or incorporated into "memory tools," which are lowered into the borehole on steel or alloy wires. Fiber-optic cables can also be inserted into boreholes to provide synoptic temperature profiles or a time series of profiles.

A variety of techniques, based on both steady-state and transient heat flow, can be used to characterize the thermal conductivity of rock specimens. Optical scanning methods provide rapid estimates of thermal conductivity and are valuable reconnaissance tools complementary to the conventional techniques.

Bibliography

Antriasian, A. M., 2010. The Portable Electronic Divided Bar (PEDB): a tool for measuring thermal conductivity of rock samples. In *Proceedings, World Geothermal Congress 2010*, Bali, Indonesia, 25–29 April 2010. 7 pp. See also http://www.hotdryrocks.com/content/view/130/73/

Beardsmore, G. R., and Cull, J. P., 2001. *Crustal Heat Flow: A Guide to Measurement and Modeling*. Cambridge: Cambridge University Press, 324 pp.

Beck, A. E., 1957. A steady-state method for the rapid measurement of the thermal conductivity of rocks. *Journal of Scientific Instruments*, **34**, 186–189.

Blackwell, D. D., and Steele, J. L., 1989. Thermal conductivity of sedimentary rocks: measurements and significance. In Naeser, N. D., and McCulloh, T. H. (eds.), *Thermal History of Sedimentary Basins*. New York: Springer, pp. 13–36.

Burkhardt, H., Honarmend, H., and Pribnow, D., 1990. *First Results of Thermal Conductivity Measurements with a Borehole Tool for Great Depths, KTB Report 90–6a*. New York: Springer, pp. 245–258.
Doig, R., Saull, V. A., and Butler, R. A., 1961. A new borehole thermometer. *Journal of Geophysical Research*, **66**, 4263–4264.
Förster, A., Schrötter, J., Merriam, D. F., and Blackwell, D. D., 1997. Application of optical-fiber temperature logging – an example in a sedimentary environment. *Geophysics*, **62**, 1107–1113.
Freifeld, B. M., Finsterle, S., Onstott, T. C., Toole, P., and Pratt, L. M., 2008. Ground surface temperature reconstructions: using *in situ* estimates for thermal conductivity acquired with a fiber-optic distributed thermal perturbation sensor. *Geophysical Research Letters*, **35**, L14309, doi:10.1029/2008GL034762.
Henninges, J., Zimmermann, G., Büttner, G., Schrötter, J., Erbas, K., and Huenges, E., 2005. Wireline distributed temperature measurements and permanent installations behind casing. In *Proceedings World Geothermal Congress*, Antalya, Turkey, 24–29 April 2005, 5 pp.
Horai, K. I., 1971. Thermal conductivity of rock-forming minerals. *Journal of Geophysical Research*, **76**, 1278–1308.
Ito, Y., Saito, T., and Nagumeo, M., 1977. Shotherm QTM measurement of Rock Specimens, Shotherm Sales Information #111: Abstracted and translated with permission from the original paper in Japanese:Shotherm QTM measurement of Rock Specimens, *Chinetsu*, 14, 21.
McGee, and Thomas, D., 1988. *Principles and Methods of Temperature Measurement*. New York: Wiley-Interscience, 608 pp.
Popov, Y. A., Pribnow, D. F. C., Sass, J. H., Williams, C. F., and Burkhardt, H., 1999. Characterization of rock thermal conductivity by high-resolution optical scanning. *Geothermics*, **28**, 253–276.
Pribnow, D. F. C., and Sass, J. H., 1995. Determination of thermal conductivity for deep boreholes. *Journal of Geophysical Research B*, **100**, 9981–9994.
Sass, J. H., Lachenbruch, A. H., and Munroe, R. J., 1971. Thermal conductivity of rocks from measurements on fragments and its application to heat-flow determinations. *Journal of Geophysical Research*, **76**, 3391–3401.
Sass, J. H., Kennelly, J. P., Jr., Wendt, W. E., Moses, T. H., Jr., and Ziagos, J. P. 1979. In Situ determination of heat flow in unconsolidated sediments, *U.S. Geological Survey Open-File Report,* 79–593, 73pp. Available in digital form as http://pubs.er.usgs.gov/usgspubs/ofr/ofr79593
Sass, J. H., Kennelly, J. P., Wendt, W. E., Moses, T. H., Jr., and Ziagos, J. P., 1981. *In situ* determination of heat flow in unconsolidated sediments. *Geophysics*, **46**, 76–83.
Sass, J. H., Kennelly, J. P., Jr., Smith, E. P., and Wendt, W. E., 1984. Laboratory line-source methods for the measurement of thermal conductivity of rocks near room temperature. *U.S. Geological Survey Open-File Report*, 84–91, 20pp. Available in digital form as http://pubs.er.usgs.gov/usgspubs/ofr/ofr8491
Selker, J. S., Thévenaz, L., Huwald, H., Mallet, A., Luxemburg, W., van de Giesen, N., Stejskal, M., Zeman, J., Westhoff, M., and Parlange, M. B., 2006. Distributed fiber-optic temperature sensing for hydrologic systems. *Water Resources Research*, **42**, W12202, doi:doi:10.1029/2006WR005326.
Suto, Y., Sakuma, S., Takahashi, H., Hatakeyama, N., and Henfling, J., 2008. Temperature memory gauge survey and estimation of formation temperature of the USDP-4 conduit hole at Unzen Volcano, Japan. *Journal of Volcanology and Geothermal Research*, **175**(1–2), 20–27.
Tew, W. L., and Strouse, G. F., 2001. Standard Reference Material 1750: Standard Platinum Resistance Thermometers, 13.8033 K to 429.7485 K, NIST Special Publication 260–139, U.S.Government Printing Office, Washington, D.C., 37 pp. Specific information on RTD devices is best obtained by entering "resistance temperature devices" into an Internet Search Engine. An excellent contemporary source is http://www.omega.com/temperature/Z/TheRTD.html).

Cross-references

Heat Flow, Continental
Heat Flow, Seafloor: Methods and Observations
Thermal Storage and Transport Properties of Rocks, I: Heat Capacity and Latent Heat
Thermal Storage and Transport Properties of Rocks, II: Thermal Conductivity and Diffusivity

HEAT FLOW, CONTINENTAL

Paul Morgan
Colorado Geological Survey, Denver, CO, USA

Synonyms

Heat flow; Heat flow density; Heat flux, land; Terrestrial heat flow

Definition

Heat flow. The outward flow of thermal energy by conduction from within the Earth through the solid surface of the Earth.
Continental heat flow. Heat flow from the continental crust or lithosphere, which are those portions of the plates that are not directly formed by seafloor spreading at mid-ocean ridges and are not generally subducted.

Introduction

Heat flow is a fundamental property of the Earth. The Earth is a heat engine that drives plate tectonics and intraplate processes such as hot-spot volcanism unrelated to plate margins. Heat flow, the outward flow of thermal energy from within the Earth through the solid surface of the Earth, is a measure of the thermal energy that drives this heat engine. In addition, temperature in the Earth, which is closely related to heat flow, is a primary parameter controlling physical properties of materials within the Earth. In general, areas of high heat flow are underlain by higher temperatures, at least at shallow depth, than areas of low heat flow. We seek therefore to know the distribution of heat flow from the surface of the Earth and to understand the factors that control its variations.

The primary factor controlling the distribution of heat flow is the type of lithosphere, continental or oceanic. Continental lithosphere is generally relatively old (>500 Ma) and the dominant mechanism of heat transfer through this lithosphere is conduction. A significant portion of heat flow from this lithosphere is generated by radiogenic heat production in the continental crust. In contrast, oceanic lithosphere is young (<200 Ma), heat is convected into this lithosphere as it is formed at mid-ocean ridges and it has very little internal radiogenic heat production (see *Heat Flow, Seafloor: Methods and Observations*). A variety of

geologic processes modify continental lithosphere and most of these processes also modify the thermal regime. In addition, the upper continental crust commonly hosts moving groundwater that redistributes heat in the upper crust. Thus, the long and complex history of continental lithosphere, significant and lateral variability in radiogenic heat generation, and redistribution of heat by groundwater combine to make continental heat flow heterogeneous.

Fourier's law

Under conditions of steady state, heat flow, q, is a function of thermal conductivity, K, and temperature, T, given by Fourier's law:

$$q = -K\nabla T, \tag{1}$$

where ∇ is the gradient operator. This equation assumes that thermal conductivity is isotropic, that is, it does not change with direction. In general, spatial changes in thermal conductivity and anisotropy must be considered. The negative sign in the equation recognizes that heat flows from higher temperatures to lower temperatures and that flow of heat is in the opposite direction to the temperature gradient. On average, Earth heat flow is primarily vertical and the vertical component of heat flow, q_z, is commonly quoted:

$$q_Z = -K\frac{\partial T}{\partial z}, \tag{2}$$

where z is depth. In practice, the subscript and negative sign are commonly omitted:

$$q = K\,\partial T/\partial z. \tag{2a}$$

The working units of q, K, and $\partial T/\partial z$ are $\mathrm{mW\,m^{-2}}$, $\mathrm{W\,m^{-1}\,^{\circ}C^{-1}}$ or $\mathrm{W\,m^{-1}\,K^{-1}}$, and $\mathrm{^{\circ}C\,km^{-1}}$, respectively.

Under transient conditions the heat conduction equation in one dimension becomes:

$$\frac{\partial T}{\partial t} = \kappa\frac{\partial^2 T}{\partial z^2}, \tag{3}$$

where t is time and κ is thermal diffusivity, given by $\kappa = K/\rho c$, where ρ is density and c is specific heat. The general working units for t and κ are s and $\mathrm{mm^2\,s^{-1}}$, although Ma and $\mathrm{km^2\,Ma^{-1}}$ are also sometimes used.

If heat generation, A, is also included, the heat flow equation becomes:

$$\frac{\partial^z T}{\partial z^z} - \frac{1}{\kappa}\frac{\partial T}{\partial t} + \frac{A}{K} = 0. \tag{4}$$

The working units for radiogenic heat generation, A, are $\mu\mathrm{W\,m^{-3}}$.

Geothermal gradient

The rate of increase in temperature with depth, $\partial T/\partial z$, is the *geothermal gradient*. This term is usually reserved for zones over which heat is transferred by conduction and the rate of increase in temperature with depth is linear (see *Heat Flow Measurements, Continental*), but if detailed temperature data are not available or gradients are estimated from oil-well bottom-hole temperatures, an approximate average geothermal gradient may be given. The profile of temperature plotted as a function of depth is the *geotherm*.

Geothermal gradients range from very low to near zero in fore-arc regions, the zones between subduction zones and their associated volcanic belts where heat is convected downward by the subducting lithosphere. Similarly, low gradients are found in zones of groundwater recharge. Gradients in excess of $20{,}000^{\circ}\mathrm{C\,km^{-1}}$ have been measured at one location in the upper few meters of the sediments beneath Yellowstone Lake inside the caldera of Yellowstone National Park, Wyoming, USA (Morgan, et al., 1977), but such high gradients are buffered by the boiling point curve of water as soon as temperatures reach the boiling temperature at depth. Thus, there is a very wide range of geothermal gradients in the upper continental crust. Temperatures are ultimately controlled by the boiling point curve of water in the uppermost crust and then the solidus curves of the crust and mantle lithosphere, and temperatures at depth generally do not range as widely as shallow geothermal gradients might suggest. Thermal conductivity varies by a factor of about 5 in the main rock types that comprise the continental crust (see *Thermal Storage and Transport Properties of Rocks, I: Heat Capacity and Latent Heat*): there is some variation in heat flow associated with changes in thermal conductivity, but the most significant variations in heat flow are accompanied by changes in geothermal gradient.

Sources of heat

There are two sources of heat contributing to continental heat flow, heat that enters continental lithosphere from below, and heat generated within the continental lithosphere (see *Energy Budget of the Earth*). Although the Earth beneath the lithosphere has thermal energy that must ultimately be lost to the surface either through the lithosphere or in the process of the formation of new oceanic lithosphere at mid-oceanic ridges, there is no requirement where or when that heat must be lost, that is, there is no constant basal heat flux that flows into continental lithosphere. The thermal boundary condition at the base of the lithosphere is probably more accurately described as a constant temperature boundary, and this constant temperature may be maintained either by small-scale convection and/or lateral flow in the asthenosphere. Heat flow into the base of the lithosphere is then determined by the thermal conductivity structure of the lithosphere, the thickness of the lithosphere, heat production within the lithosphere, and its surface temperature. The resulting thermal profile is disrupted during major deformation of the lithosphere or changes in its boundary conditions.

By far the largest source of heat within the lithosphere is radiogenic heat production from the decay series of

the unstable isotopes ^{232}Th, ^{235,238}U, and ^{40}K. These isotopes all have half-lives of the same order as the age of the Earth and thus remain sufficiently abundant to be significant and continue to decay at a rate that is significant in terms of heat production (see *Radiogenic Heat Production of Rocks*). Other radiogenic isotopes are important for age dating, such as ^{87}Rb, ^{147}Sm, and ^{187}Re (see *Absolute Age Determinations: Radiometric*), but the heat produced by the decay of these isotopes and other isotopes used for age dating is insignificant. Uranium, thorium, and potassium are incompatible elements and tend to be concentrated in silicic magmas. Hence, they are depleted in the mantle during crustal formation and generally concentrated in the crust in silicic rocks. Heat flow data show that their concentrations in large silicic plutons are relatively predictable from surface measurements (Roy et al., 1968), but their distributions are less predictable in metamorphic and sedimentary terrains (see *Lithosphere, Continental: Thermal Structure*). Measurements indicate that from as little as less than 20% to as much as 80% of heat flow may be derived from crustal radiogenic heat generation. Typical values of heat production for crustal rocks range from $<0.1\ \mu W\,m^{-3}$ for basic igneous rocks to $>6\ \mu W\,m^{-3}$ for radiogenic granites.

Other crustal heat sources include frictional heat from faults and heat from chemical reactions. Attempts to measure heat associated with active faults have generally failed to detect heat or produced inconclusive results. The primary chemical reaction that has been observed as a heat source is the oxidation of pyrite, but any exothermic metamorphic or weathering reaction is a potential heat source. However, friction and chemical heat sources are likely to be only local in extent and minor in terms of the total continental thermal budget.

Mechanisms of heat transport

In stable continental crust, the primary mechanism of heat transfer is conduction as described by Fourier's law (Equations 1 and 2). In the mantle, the effects of radiative heat transfer may be significant as olivine has a significant component of radiative heat transfer above a temperature of about 500°C. This radiative component may be included in Fourier's law by substituting a temperature-dependent value of thermal conductivity that includes a correction for radiative heat transfer.

Even in stable regions, heat may be redistributed in the upper few kilometers by groundwater flow. In stable regions the geothermal gradient is seldom high enough to drive free convection (see below), and groundwater flow is driven by differences in elevation of the piezometric surface (water table). Heat transferred by the forced vertical flow of groundwater, q_{gw}, may be approximated by:

$$q_{gw} = \bar{v} c_w |dT|, \tag{5}$$

where $\bar{v}$ is the equivalent vertical velocity if the porosity were 100%, c_w is the specific heat of water, and $|dT|$ is the absolute temperature drop over the vertical extent of the water flow. Heat transfer will be in the direction of water flow and heat flow is decreased in areas of recharge and increased in areas of discharge. This type of convection is termed forced convection or advection.

If the geothermal gradient is sufficiently high, water flow may be driven by thermal buoyancy forces. The magnitude of the gradient required for the onset for thermal convection depends on the geometry of the heat source and the medium in which convection occurs (e.g., Turcotte and Schubert, 2002, p. 393 et seq.). For a homogeneous porous layer of permeability $k\,m^2$ and thickness b km heated uniformly from below, the minimum thermal gradient, $(\partial T/\partial z)_{min}$, required for convection to occur is given by:

$$\left(\frac{\partial T}{\partial z}\right)_{min} = \frac{4.2x10^{-10}}{kb^z}. \tag{6}$$

This minimum gradient may not sustain convection and a higher gradient may be required for continuous convection. Convection driven by thermal buoyancy forces is termed free convection.

Heat will also be convected when there are net vertical movements within the lithosphere associated with deformation or changes in either the top or bottom boundaries of the lithosphere. In general, extensional deformation causes thinning of the lithosphere resulting in a net upward movement of the material in the lithosphere relative to its surface and a compression of the isotherms, or horizons of equal temperature within the lithosphere (Figure 1a). In contrast, compressional deformation causes thickening of the lithosphere resulting in a net downward movement of the material in the lithosphere relative to its surface and an increase of the spacing of the isotherms within the lithosphere (-Figure 1b). For simplicity, deformation in Figure 1 is shown to be 100% by pure shear and uniformly distributed throughout the lithosphere, a highly unlikely distribution of geological strain. As shear strength changes from brittle to ductile laterally and with depth throughout the lithosphere, the strain distribution is always much more complex: zones of simple shear, imbricated layers, and other complexities typically characterize lithospheric deformation. However, at a lithospheric scale, the net material movements and compression and extension of the geotherms illustrated in Figure 1 are valid.

Stable continental lithosphere has a relatively low heat flow corresponding to a low geothermal gradient and strong lithosphere. These conditions are not favorable for deformation. Observations indicate that deformation commonly occurs in lithosphere that is still recovering from a previous thermal event or has experienced a preceding thermal event. This thermal event may be manifested in the form of volcanism in which heat is advected in the lithosphere by ascending magmas. Heat transfer by magmas is conceptually similar to heat transfer by groundwater described by Equation 5, if the specific heat of magma is substituted for the specific heat of water. Additional heat is released from a magma during

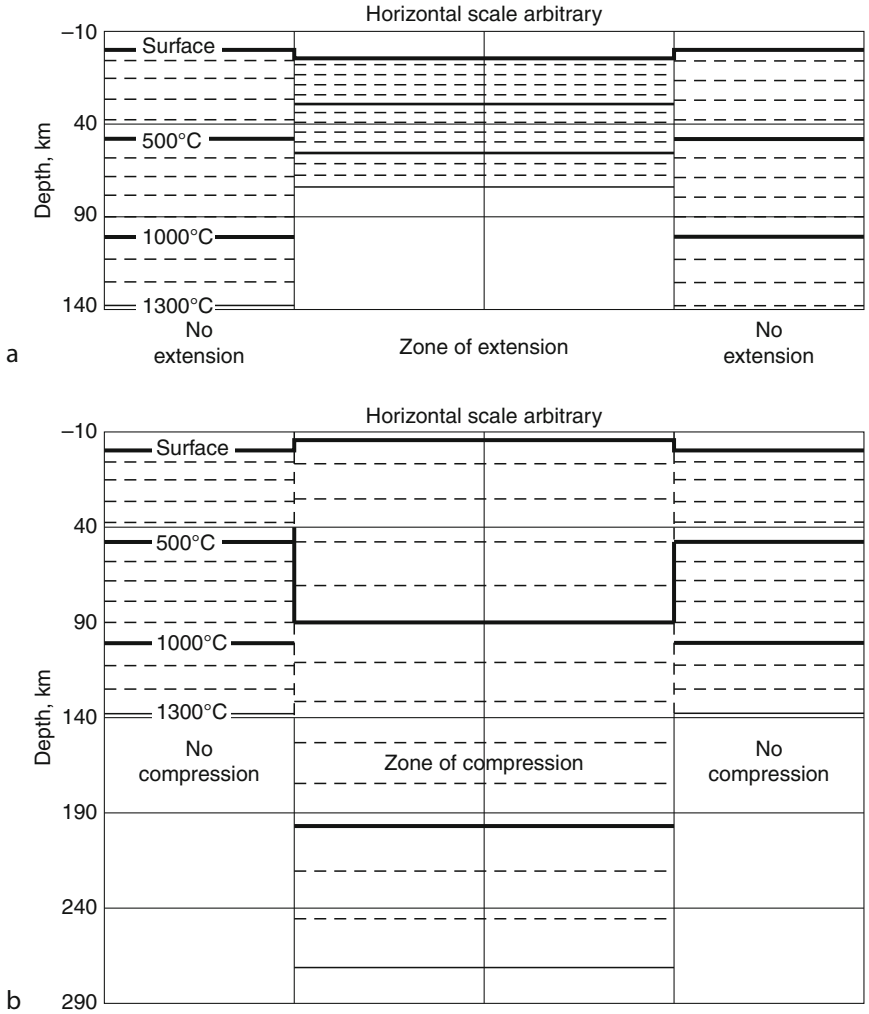

Heat Flow, Continental, Figure 1 Diagrammatic examples of the effects of instantaneous pure shear deformation on lithospheric isotherms. Both diagrams have the same thermal conditions in undeformed lithosphere (no extension and no compression) calculated for a 35 km thick crust with a surface heat flow of 40 mW m^{-2}, a surface heat production of 2 μW m^{-3}, and a crustal thermal conductivity of 2.5 W m^{-1} K^{-1}. The crustal heat production is assumed to decay exponentially with depth with a depth parameter of 10 km, and the mantle is assumed to have a heat production of 0.084 μW m^{-3} and a temperature-dependent thermal conductivity appropriate for olivine. The base of the lithosphere is assumed to be the 1,300 °C isotherm. (**a**) shows the effect of thinning the lithosphere by a factor of 2 by extending the lithosphere by a factor of 2. (**b**) shows the effect of doubling the thickness of the lithosphere by compressing the lithosphere by a factor of 2.

solidification, and this heat is represented by the latent heat of solidification. Many analytical solutions for conductive modeling of magma intrusions may be found in Carslaw and Jaeger (1959) and other references, and these processes may also be modeled numerically. Magma generation may be initiated from below the lithosphere by the ascent of hot material to the base of the lithosphere (mantle plumes?) generating magmas by pressure-release melting and raising the temperature at the lower boundary of the lithosphere. Additionally magmas may be generated within the lithosphere by pressure-release melting and the melting of lower-melting temperature components within the lithosphere.

Once deformation is initiated additional magma generation will be initiated. The net upward movement of material during extension may trigger pressure-release melting, especially if the lithosphere has been preheated by pre-deformation magmatism. During compression, there is a net syn-deformational lowering of the geotherm. However, thickening of the crustal layer of radiogenic heat-producing elements will generally cause the geothermal gradient to return to a higher value than its initial value. This higher geotherm may result in melting of the thickened crust and crustal derived magmatism, the results of which are commonly observed in belts of compressional deformation. Thus, magmatic

convection of heat is an important heat transfer mechanism that commonly accompanies heat convection by tectonic deformation.

Finally, there is heat convection associated with changes at the Earth's surface. In discussing deformation and magmatism, the effects of these processes on surface elevation were ignored. Cooling oceanic lithosphere as it ages away from oceanic ridges results in a relatively simple change in depth of the ocean floor (see *Heat Flow, Seafloor: Methods and Observations*). A similar, but more complex relation exists for the thermal and density structure of continental lithosphere (Lachenbruch and Morgan, 1990; *Isostasy, Thermal*). Changes in surface elevation are generally accompanied by either erosion or sedimentation with the net result that the material in the lithosphere has a net movement either up or down relative to the surface, respectively. If the rates of erosion or sedimentation are known, a correction may be applied for these effects. If erosion creates three-dimensional topography, a terrain correction may also be applied. Not strictly a heat transfer mechanism, but changes in surface temperature associated with past climate change or changes in land use may also change surface heat flow and a correction may be applied for these perturbations.

The duration of a thermal disturbance associated with thermal convection in the lithosphere depends primarily on the stable thickness of the lithosphere and its thermal diffusivity. There is no standard for defining this duration as temperatures relax asymptotically to their stable values, and the form of this return depends on the structure of the thermal disturbance, which may be highly variable and very complex in continental deformation with magmatism. However, a useful guideline for the duration of the thermal disturbance, τ, is:

$$\tau = \frac{L^z}{4\kappa} \tag{7}$$

where L is the stable thickness of the lithosphere and κ is its thermal diffusivity. For example, using an average thermal diffusivity of 32 $km^2\ Ma^{-1}$ and a thickness of 100 km for stable oceanic lithosphere, the calculated duration of the thermal disturbance is about 78 Ma. Oceanic crust is observed to flatten at about 70–80 Ma. For continental lithosphere, if the stable thickness of this lithosphere is 100 km, the duration of the thermal disturbance would be about 78 Ma; if the stable thickness were 150 km, the duration would be ~175 Ma; if the thickness were 200 km, the duration would be ~310 Ma; and if the stable thickness were 250 km, the duration would be ~500 Ma. These durations are from the start of stabilization: if a deformation and magmatism event were followed by significant erosion or sedimentation, the duration of the thermal stabilization would not begin until the end of the erosion or sedimentation. However, as the effects of sedimentation and erosion are relatively minor, their measurable effects would probably be dissipated before the end of the formal disturbance duration.

Global distribution of continental heat flow

The global distribution of continental heat flow is shown in Figure 2a. The density of data is far from uniform (Figure 2b), but there are sufficient data that some generalizations about the heat flow distribution may be made. In general, high heat flow corresponds with zones of active seismicity, which in turn correlate with plate margins. Where the zones of seismicity are diffuse, such as the western US and the Himalaya, the plate margin deformation is distributed and the zones of high heat flow are extensive. Some portions of active plate margins are associated with low heat flow, such as the western margin of South America and the Pacific Northwest of the USA, west of the volcanic Cascade Range. These areas overlie subducting oceanic lithosphere where heat is being convected down into the mantle. Associated with these low heat flow zones is a rapid lateral transition to high heat flow in the active volcanic zones of the subduction zones. In addition, plate margins are generally associated with elevated topography, which received more precipitation than low elevations and in which heat flow is generally more variable because of redistribution of heat by forced and free groundwater convection.

The association of high and low heat flow with active plate margins is demonstrated in a plot of mean heat flow as a function of age of heat flow site (Figure 3). Data are shown for sedimentary and metamorphic sites in Figure 3a and igneous sites in Figure 3b. The data for sedimentary and metamorphic sites (Figure 3a) show a small decrease from Cenozoic and Mesozoic to Paleozoic sites and from Paleozoic to Proterozoic sites, and a larger decrease from Proterozoic to Archean sites. This result suggests that the plate margin disturbances are relatively minor in the Phanerozoic sedimentary and metamorphic site data. In the igneous site data (Figure 3b), however, there is a significant decrease in both the mean and standard deviation from both Cenozoic to Mesozoic and from Mesozoic to Paleozoic sites. There is almost no difference in the mean from Paleozoic to Proterozoic sites. The data are the same for Proterozoic and Archean sites as Figure 3a. The igneous site data clearly show thermal perturbations with ages extending into Mesozoic age sites relative to older sites. This result is consistent with a continental lithospheric thickness of the order of 200 km. The observation that the igneous site data show a perturbation at young ages but there is only a small signal in the sedimentary and metamorphic site data suggests that the sedimentary and metamorphic site data are dominated by sedimentary sites and that these sites are either distant from plate boundaries or high heat flow is suppressed at these sites by downward advection of heat by advection during sedimentation.

The difference between the mean heat flow at Proterozoic and Archean sites has be commented upon from previous compilations of global heat flow data (Morgan, 1985) in addition to this data set (Artemieva and Mooney, 2001). To explain this difference as a transient effect would require a lithosphere of the order of 500–600 km

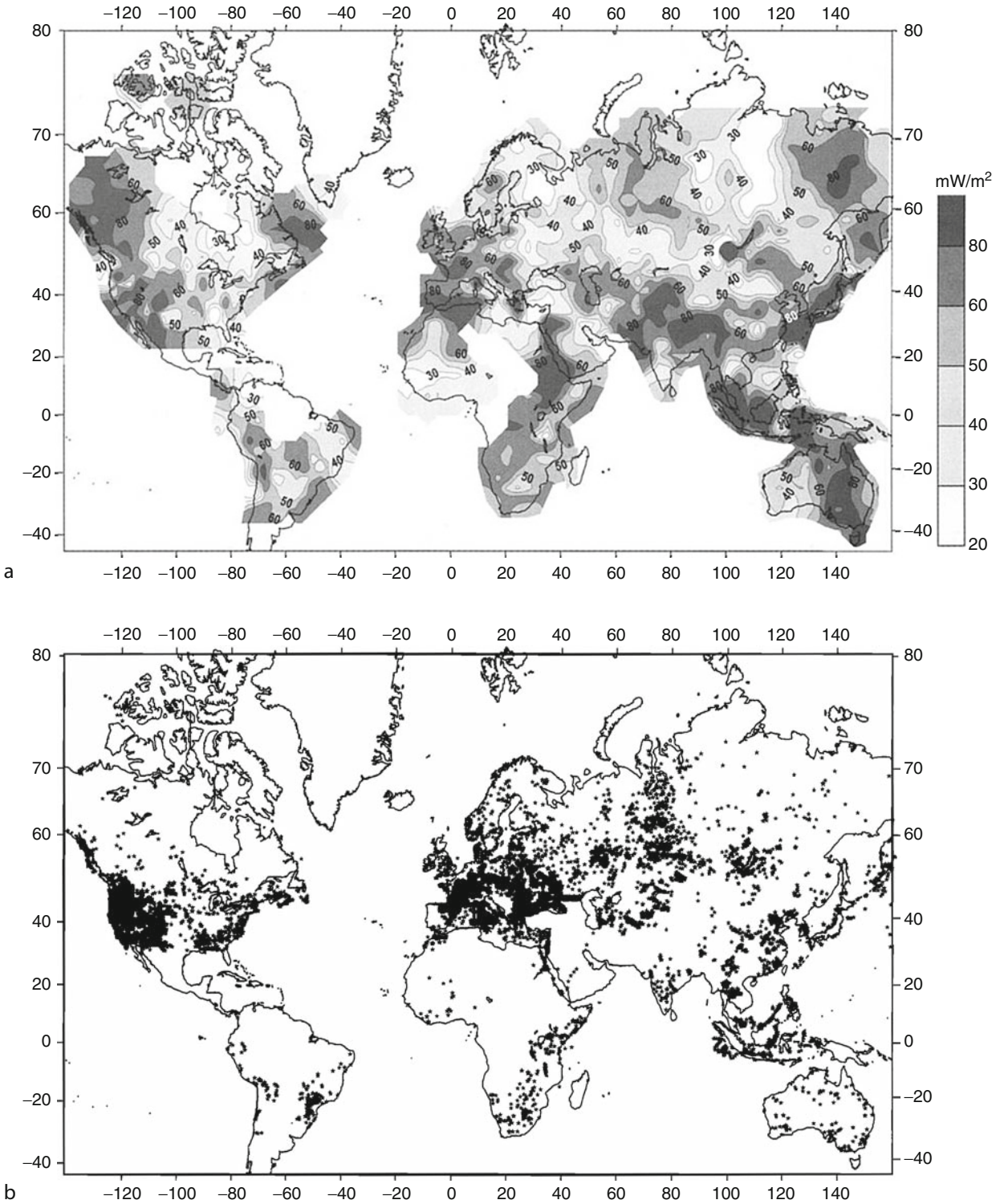

Heat Flow, Continental, Figure 2 (**a**) Distribution of continental heat flow, based on the data of Pollack et al. (1993) and subsequent updates, presented with a 10° × 10° interpolation (Artemieva and Mooney, 2001, Figure 3). (**b**). Locations of continental heat flow measurements used in constructing Figure 2(**a**) (From Artemieva and Mooney, 2001, Figure 4).

in thickness, which is probably unrealistic. However, a mean heat flow difference of 7 $mW\,m^{-2}$ may be explained in terms of a difference in the contributions of the mean heat production of Proterozoic and Archean crusts to their heat flows. Assuming an average crustal thickness of 35 km, an average difference of 0.2 $\mu W\,m^{-3}$ would explain the difference between the mean measured heat flow at Archean and Proterozoic sites. This difference is not universally observed in all areas (Jaupart and Mareschal, 1999; *Lithosphere, Continental: Thermal Structure*), but it is consistent with bulk observations of the differences in chemistry between the upper crust of Proterozoic and Archean terrains (McLennan et al., 2006). Archean upper crust is statistically depleted in the heat-producing elements relative to younger crust. In addition, xenolith data indicate that Archean lithosphere is statistically distinct from younger lithosphere so the upper crustal thermal observation may indicate that Archean lithosphere is statistically thermally distinct (Griffin et al., 2009).

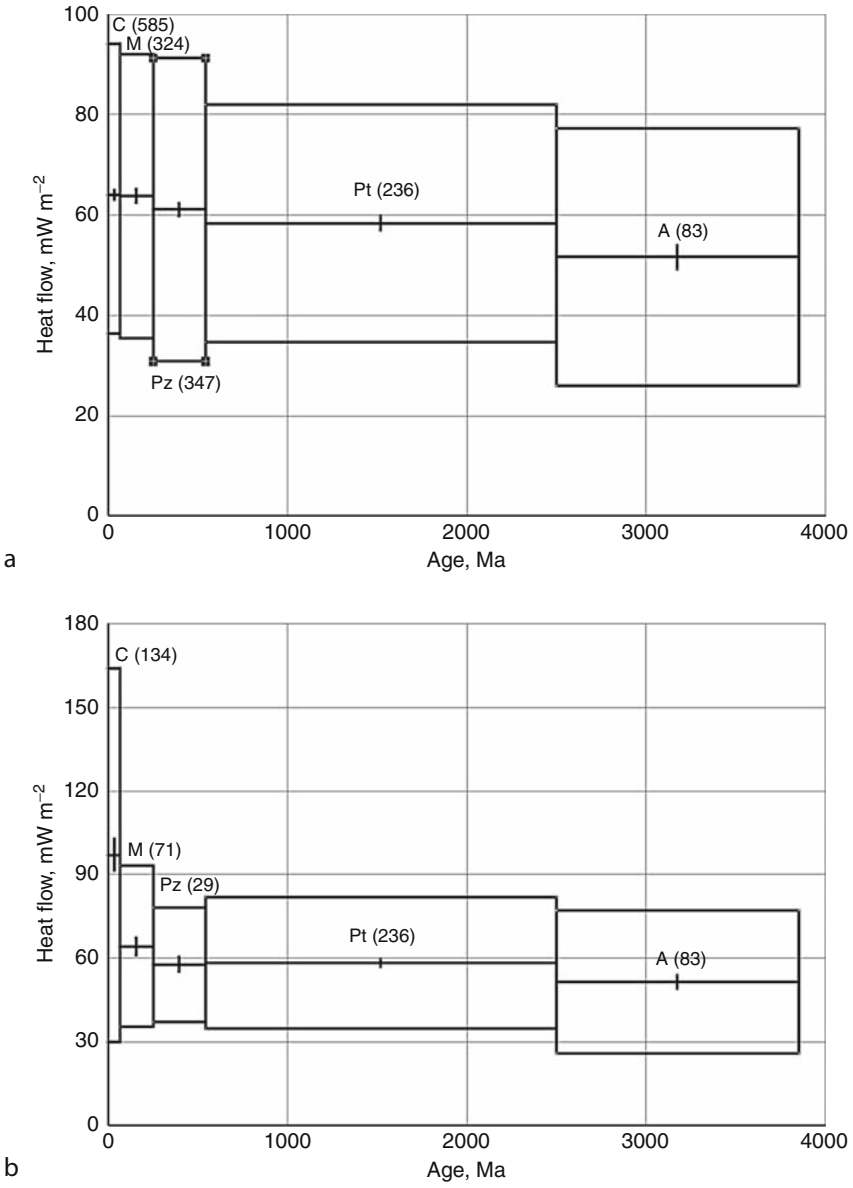

Heat Flow, Continental, Figure 3 Continental heat flow as a function of age of data site. Widths of boxes and bars indicate age range. Heights of boxes indicate ± one standard deviation about the mean; short vertical line indicates ± one standard error about the mean. Ages of sites are grouped as C – Cenozoic, M – Mesozoic, Pz – Paleozoic, Pt – Proterozoic, and A – Archean. Numbers in parentheses are the number of 1° by 1° blocks represented in each age group. (**a**) shows sedimentary and metamorphic sites for Phanerozoic data. (**b**) shows igneous sites for Phanerozoic data. Data re-plotted from Pollack et al. (1993).

In summary, the global distribution of continental heat flow is complex. Neglecting measurement errors (see *Heat Flow Measurements, Continental*), variations associated with surface temperature changes, uncorrected topographic effects, and anomalies induced by changes in surface cover, heat flow may be described as steady state or transient. At any site, near-surface heat flow may be redistributed by groundwater flow, but this is most likely at sites with high elevation and rugged topography that are likely to have experienced relatively young (Cenozoic or Mesozoic) mountain building and/or igneous activity. Transient thermal perturbations in the lithosphere associated with tectonic deformation and/or igneous activity will dissipate with time and are likely to be restricted to heat flow sites in lithosphere with Cenozoic or Mesozoic tectonic or thermal ages. To distinguish tectonic and igneous ages from sedimentary ages, the term *tectonothermal age* is commonly used to describe the age of heat flow sites. Data from sites with tectonothermal ages Paleozoic and older are generally expected to be in steady state unless erosion or sedimentation are significant.

Igneous activity always heats continental lithosphere but deformation may either raise or lower the geothermal gradient (Figure 1). There is therefore no predictable anomaly for continental lithosphere at or near plate margins. The wide range in observed heat flow measured at young sites is in part associated with redistribution of heat by groundwater flow, but also associated with the real range in anomalies, both positive and negative, generated by deformation.

Whether the heat flow and geotherm be transient or steady state, significant variation among sites may occur associated with crustal radiogenic heat generation. Heat generation in the upper crust is very variable being generally low in mafic rocks and high in silicic rocks. Its contribution may vary from $<20\%$ to $>70\%$ of heat flow, and much of the range in heat flow represented in the standard deviations about the means of heat flow in Figure 3 are probably associated with chemical heterogeneity in the continental crust resulting in lateral variations in the contributions of radiogenic heat production to heat flow.

Paleo-heat flow

The discussion above has been restricted to heat flow measured at present although there is some lag in heat flow measured at the surface as it is conducted from depth: the order of that time lag may be estimated from Equation 7. This heat flow and associated temperatures are appropriate for most use for geophysical parameters, such as seismic wave velocities, electrical conductivities, and density calculations, but the time lag may be significant in some area where temperatures at depth in the lithosphere are changing. However, for some geological observations, including most techniques of radiometric age dating, the former temperature of a rock or mineral are preserved in a chemical or radiometric system when the rock cools as it is brought to the surface. This process may allow the temperature and sometimes the geothermal gradient of a site to be reconstructed at the time the rock was uplifted and this general topic is sometimes referred to as paleo-heat flow.

The rates of most chemical reactions increase at higher temperatures. For example, the maturation of organic material in sediments roughly follows the Arrhenius' equation, which describes the velocity of the reaction, r, as:

$$r = \lambda \exp(-E/RT_K) \tag{8}$$

where λ is the frequency factor, E is the activation energy, R is the gas constant, and T_K is temperature in Kelvin (Stegena, 1988). The combination of the frequency factor and temperature gives a time-temperature index that, together with composition of the organic matter, provides a useful predictor of hydrocarbon maturation. Temperatures in sedimentary basins are usually estimated by the increase in coal rank of carbonaceous matter in the sediments as measured by its vitrinite reflectance (e.g., Suggate, 1998), and time may be estimated by the sedimentation history of the basin. Vitrinite reflectance measures the maximum temperatures attained by the sediments, which may exceed modern temperatures.

Radiometric methods for age dating (see *Absolute Age Determinations: Radiometric*) do not determine rock ages but the time at which the radiometric system on which the age determination is based cools through its closure temperature, the temperature at which the age is set. Thus, radiometric ages may be used for the additional purpose of determining the thermal history of a rock, especially if some estimate of the depth at which the age was set may be determined (see below). Radiometric systems do not close at a single temperature but follow the Arrhenius' equation; at high temperatures cooling is generally relatively rapid. Examples of approximate mineral-closure temperatures for the uranium-lead method are monazite $>1{,}000°C$, zircon $>1{,}000°C$, titanite 650–600°C, apatite 500–450°C, and rutile 450–400°C (Flowers, 2005). Examples of approximate mineral-closure temperatures for the potassium-argon system are hornblende $530 \pm 40°C$, muscovite $\sim 350°C$, and biotite $280 \pm 40°C$ (McDougall and Harrison, 1999). Different dates from these minerals may be used to calculate rates of erosion or exhumation of terrains. However, young ages may also indicate reheating for minerals with relatively low-temperature closure temperatures.

The minerals used for some radiogenic systems have geologically very low closure temperatures. For example, the fission track technique is based on radiation damage (tracks) in different minerals caused by the spontaneous fission of ^{238}U (Garver, 2008). Closure of this system is by thermal annealing of the fission tracks, which occurs at $>120°C$ for apatite, $\sim 200°C$ for zircon, and $\sim 300°C$ for sphene. At these low temperatures, a geothermal gradient is usually assumed and the fission track ages are commonly used to indicate recent uplift/erosion rates (uplift/erosion rate = closure temperature/[fission track age × assumed geothermal gradient]).

Finally, paleo-thermal conditions are preserved by metamorphism, and in particular in mineral systems called geothermometers. Geothermometers are typically pairs of minerals in which concentration of one element in one of the minerals has a strong temperature dependence but is essentially pressure independent; the other mineral, which must be in intimate contact with the first mineral grain, acts as a reservoir for this element and allows the first mineral to be in thermal equilibrium with the element. Geothermometers tend to equilibrate rapidly at high temperatures but re-equilibrate slowly as the temperature decreases, so if cooling and exposure at the surface is relatively rapid, the geothermometer records peak thermal conditions. Geobarometers also exist in which the concentration of an element in the first mineral is strongly pressure (depth) dependent but insensitive to temperature. If mineral pairs representing a geothermometer and a geobarometer occur in the same outcrop, then temperature and depth may be estimated allowing calculation of the paleo-geothermal gradient and heat flow at the time of peak thermal conditions.

Studies of paleo-thermal gradients from metamorphic terrains suggest that, on average, geothermal gradients were higher than modern average geothermal gradients. However, although global heat flow was almost certainly higher in the past than at present (see *Energy Budget of the Earth*), these observations do not demonstrate that conclusion for the following reasons: (1) only peak or near-peak thermal conditions are preserved resulting in an overestimation of average continental heat flow; (2) peak preserved geothermal gradients are no higher than geothermal gradients measured today – modern geothermal gradients are buffered in the uppermost crust by the water boiling point curve and at greater depths by the crust solidus, and the same conditions would have applied in the earliest Earth preserved in the continental crust; and (3) if there were zones of low temperature/high pressure metamorphism (blueschist) in the Archean/Early Proterozoic, they are unlikely to be preserved because a geotherm required to maintain these metamorphic conditions requires active subduction. With the cessation of subduction, the geotherm would relax to a warmer geotherm, and blueschist metamorphism is likely to be overprinted. Similarly, low temperatures would not be recorded by geothermometers as the lithospheric temperatures increase.

Summary

Continental heat flow is a complex, but fundamental parameter that, together with oceanic heat flow, constrains the energy budget of the Earth heat engine. It is particularly complex because continents are complex and heterogeneous. It has components from beneath the lithosphere and radiogenic heat production within the lithosphere. Heat is advected into and within the lithosphere by magmatic activity, and heat is redistributed by lithospheric deformation associated with plate tectonics and at relatively shallow depths by groundwater flow. Changes in surface conditions also modify heat flow in the shallow crust. The time constant of thermal relaxation of continental lithosphere is of the order of 300 Ma for stable lithosphere 200 km in thickness. Typically heat flow data from igneous sites of Cenozoic and Early Mesozoic ages reflect transient thermal conditions; data from sites of older ages do not. However, continental heat flow remains very variable even at Precambrian sites because of lateral variability in crustal radiogenic heat production.

Bibliography

Artemieva, I. M., and Mooney, W. D., 2001. Thermal thickness and evolution of Precambrian lithosphere. *Journal of Geophysical Research*, **106**, 16387–16414.

Carslaw, H. S., and Jaeger, J. C., 1959. *Heat Conduction in Solids*. Oxford: Oxford University Press, 510. pp.

Flowers, R. M., 2005. Tempo of burial and exhumation within the deep roots of a magmatic arc, Fiordland, New Zealand. *Geology*, **33**, 17–20.

Garver, J. I., 2008. Fission-track dating. In Gornitz, V. (ed.), *Encyclopedia of Paleoclimatology and Ancient Environments*. Dordrecht: Springer, pp. 247–249.

Griffin, W. L., O'Reilly, S. Y., Afonso, J. C., and Begg, G. C., 2009. The composition and evolution of lithospheric mantle: a re-evaluation and its tectonic implications. *Journal of Petrology*, **50**, 1185–1204.

Jaupart, C., and Mareschal, J.-C., 1999. The thermal structure and thickness of continental roots. *Lithos*, **48**, 93–114.

Lachenbruch, A. H., and Morgan, P., 1990. Continental extension, magmatism and elevation; formal relations and rules of thumb. *Tectonophysics*, **174**, 39–62.

McDougall, I., and Harrison, T. M., 1999. *Geochronology and Thermochronology by the $^{40}Ar/^{39}Ar$ Method*. New York: Oxford University Press.

McLennan, S. M., Taylor, S. R., and Hemming, S. R., 2006. Composition, differentiation, and evolution of continental crust: constraints from sedimentary rocks and heat flow. In Brown, M., and Rusher, T. (eds.), *Evolution and Differentiation of Continental Crust*. New York: Cambridge University Press, pp. 92–134.

Morgan, P., 1985. Crustal radiogenic heat production and the selective survival of ancient continental crust. *Journal of Geophysical Research*, **90**, C561–C570. Supplement.

Morgan, P., Blackwell, D. D., Spafford, R. E., and Smith, R. B., 1977. Heat flow measurements in Yellowstone Lake and the thermal structure of the Yellowstone Caldera. *Journal of Geophysical Research*, **82**, 3719–3732.

Pollack, H. N., Hurter, S. J., and Johnson, J. R., 1993. Heat flow from the Earth's interior: analysis of the global data set. *Reviews of Geophysics*, **31**, 267–280.

Roy, R. F., Blackwell, D. D., and Birch, F., 1968. Heat generation of plutonic rocks and continental heat flow provinces. *Earth and Planetary Science Letters*, **5**, 1–12.

Stegena, L., 1988. Paleogeothermics. In Haenel, R., Rybach, L., and Stegena, L. (eds.), *Handbook of Terrestrial Heat-Flow Density Determination*. Dordrecht: Kluwer, pp. 391–419.

Suggate, R. P., 1998. Relations between depth of burial, vitrinite reflectance and geothermal gradient. *Journal of Petroleum Geology*, **21**, 5–32.

Turcotte, D. L., and Schubert, G., 2002. *Geodynamics*. Cambridge: Cambridge University Press.

Cross-references

Absolute Age Determinations: Radiometric
Energy Budget of the Earth

Heat Flow, Continental
Isostasy
Lithosphere, Continental: Thermal Structure
Lithosphere, Oceanic: Thermal Structure
Radiogenic Heat Production of Rocks
Thermal Storage and Transport Properties of Rocks, I: Heat Capacity and Latent Heat

HEAT FLOW, SEAFLOOR: METHODS AND OBSERVATIONS

Earl E. Davis[1], Andrew T. Fisher[2]
[1]Pacific Geoscience Centre, Geological Survey of Canada, Sidney, BC, Canada
[2]Earth and Planetary Sciences Department, University of California at Santa Cruz, Santa Cruz, CA, USA

Definition

Heat flow. The rate of thermal energy transfer in a medium driven either conductively along a thermal gradient or advectively via mass transport. The standard unit is watts, W. The term is also used to describe a subdiscipline of geophysics, as in the title of this entry.

Conductive heat flux. The heat flow per unit area diffusing by conduction along a thermal gradient, determined as the product of the thermal gradient and thermal conductivity. The standard unit is W m^{-2}. The term *heat flow density* has been used correctly as a synonym; the term *heat flow*, traditionally but inexactly used as a synonym for heat flux, more strictly applies to the integrated heat flux over a specified area or region (watts).

Advective heat flux. The rate of heat transfer per unit area carried by a moving medium, proportional to the velocity and the heat capacity of the medium. The standard unit is W m^{-2}.

Thermal conductivity. The quantity that defines the ability of a medium to transfer heat by steady-state diffusion. The standard unit is W m^{-1} K^{-1}.

Hydrothermal circulation. Large-scale pore-fluid convection driven by thermal buoyancy, in which fluid flux and advective heat flux are strongly influenced by the permeability structure of the host formation.

History of observations

Pioneering measurements of temperature below the seafloor (e.g., Petterson, 1949; Revelle and Maxwell, 1952; Bullard, 1954) were made to compare the thermal state of the ocean crust with that of continents and thus to improve the knowledge of the present-day heat loss from the Earth. The early data demonstrated that gravity-driven probes and corers that penetrated a few meters into seafloor sediments could provide meaningful geothermal gradients, and they provided a foundation for the marine heat flow discipline. Methods for measuring the seafloor thermal gradient and thermal conductivity (the product of which is conductive heat flux) improved in subsequent years, the number and geographic distribution of determinations increased, and patterns of seafloor heat flux were gradually revealed. Initially, the average seafloor heat flux appeared to be similar to that through continents, despite the contribution from crustal radiogenic heat production, which is significant in the continental crust but not in the oceanic crust. Heat-flux values over midocean ridges were found to be significantly higher on average than in the flanking basins, but locally, values were often inexplicably scattered (Von Herzen and Uyeda, 1963; Lee and Uyeda, 1965). Higher heat flux at midocean ridges was consistent with emerging ideas about seafloor spreading, although the values measured were lower than expected from early theoretical models for the formation of ocean lithosphere. For nearly 2 decades, regionally low and scattered seafloor heat-flux values remained unexplained.

By the 1970s, studies began to be done with improved navigation, and with more closely spaced measurements made in the context of local sediment and igneous crustal structure. Results provided a sound basis for the hypothesis that hydrothermal circulation in the igneous crust and advective loss through unsedimented igneous outcrops caused both the scatter and the lower-than-expected values in young areas (Lister, 1972). Further improvements to instrumentation and observational strategies, in particular the development of probes that could be used with great efficiency for multiple measurements during a single instrument lowering, and the practice of making measurements in the context of geologic structure, led to the use of heat flux in the study of the process of hydrothermal circulation itself (Williams et al., 1974). With this new knowledge, it was possible to decipher the variability in measurements in a way that could lead to a better quantification of deep-seated heat flux, the goal of the original marine heat flow studies, and to understand the hydrologic processes behind the perturbations. Thus began a diverse range of applications of marine heat flow over a broad range of scales. A summary of the suite of tools currently in use for these studies is provided in the next section, along with a brief description of how heat-flux determinations are made. This is followed by a few examples of data from specific studies that illustrate how data are used, and a summary of some of the major conclusions that have been made through such studies.

Methods

Shallow measurements in marine sediments

Heat flux through the seafloor is often determined using temperatures measured with a series of sensors mounted on the outside of gravity-driven corers (Figure 1a), and thermal conductivities measured on the recovered sediment cores. Depths of penetration in excess of 10 m can be achieved in soft sediment, providing a valuable check on potential perturbations from bottom-water temperature variations, although accuracy is often limited by physical disturbances caused by the coring process, by changes in the physical properties of the recovered material, by

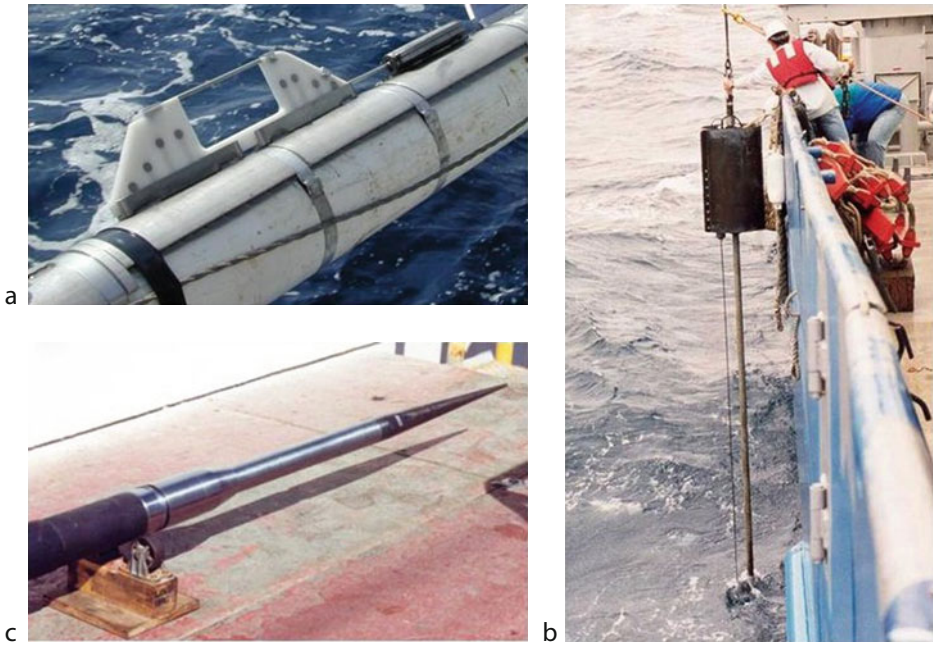

Heat Flow, Seafloor: Methods and Observations, Figure 1 Sensors and probes for measuring temperatures and thermal conductivity in marine sediments, including (**a**) outrigger temperature sensors mounted to the outside of a sediment corer (core barrel is 12 cm diameter), (**b**) a devoted heat-flux probe for measuring sediment temperatures and thermal conductivities (total length is 4.5 m), and (**c**) a high-strength probe that extends below a drill bit for bottom-hole temperature measurements (length is 1.2 m, tip diameter 1 cm).

incomplete recovery, and by the imperfect depth registration between the cores and the intervals between the temperature sensors. Probes devoted exclusively to heat-flux measurements are typically limited to lengths of a few meters, but they have several distinct advantages. They allow thermal conductivity to be measured under in situ conditions and at depths that are co-registered with temperature measurements, and they allow transects of many measurements to be made efficiently during single instrument lowerings. A typical multipenetration heat-flux probe (Figure 1b) employs a heavy strength member that resists bending during repeated penetration and withdrawal from the sediment, and a small-diameter, rapidly responding tube containing thermistor sensors and a linear heater element. In situ temperatures are estimated by extrapolating transient decays following probe penetration, and conductivities are determined from the rate of change of temperature following steady or impulsive activation of the heater. A typical data record is shown in Figure 2, as are the resulting determinations of temperature and thermal conductivity. Heat flux is determined as the linear regression fit of temperature versus cumulative thermal resistance, R:

$$R = \sum [\Delta z/\lambda(z)]$$

where λ is thermal conductivity measured at a series of depths, z, and Δz is the depth interval assumed to be represented by each measurement. This is equivalent to calculating heat flux as the product of thermal gradient and the harmonic mean of thermal conductivity between temperature measurements, as was done in early marine heat flow studies. Errors associated with possible bottom-water temperature variations are evaluated by examining systematic deviations from linearity as a function of the number of thermistors included in the fit, working progressively up toward the shallowest measurement point. Complete descriptions of instruments and discussions of data reduction methods can be found in Lister (1979); Hyndman et al. (1979); Davis (1988), Wright and Louden (1989), and Villinger and Davis (1987).

Deep borehole measurements

Where observations are needed in hard formations or at depths greater than can be penetrated with a gravity-driven device, drilling is required. For research objectives, this has been done primarily through the Deep Sea Drilling Project, the Ocean Drilling Program, and the Integrated Ocean Drilling Program. In relatively unconsolidated sediments (typically the uppermost 50–100 m below the seafloor), hydraulically driven piston corers are deployed from the bottom of the drill string, and temperatures are measured at the tip of the core barrel (Horai and Von Herzen, 1985). At greater depths below the seafloor, high-strength probes can be pushed in with the weight of the drill string sufficiently far below the bottom of the hole (c. 1 m) to gain an unperturbed measurement (Uyeda and

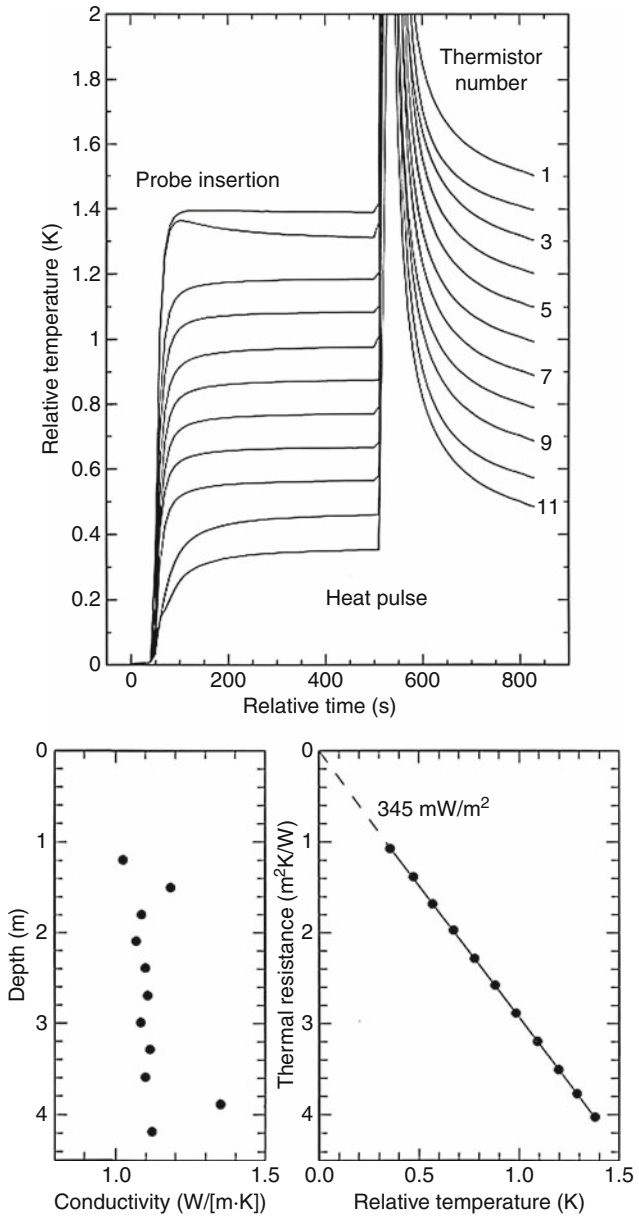

Heat Flow, Seafloor: Methods and Observations, Figure 2 Typical data (upper panel) collected with a marine heat-flux probe like that shown in Figure 1b. Thermal conductivities are determined from the rates of decay following the metered pulse of heat, and natural sediment temperatures are determined by extrapolating the transients following probe insertion. In this example, high conductivities associated with two turbididic sand layers are present.

Horai, 1980; Davis et al., 1997a) (Figure 1c). Deeper than a few hundred meters in sediment, or at any level in crystalline rock, bottom-hole measurements are not feasible; instead, long-term borehole measurements are required to discriminate the natural formation thermal state from the commonly large and long-lived perturbations from drilling and subsequent fluid flow into or out of the hole. The most reliable method for determining the natural thermal state of crustal rocks has been to seal holes and install thermistor strings for long-term monitoring (Davis et al., 1992) (Figure 3).

Example studies

Bottom-water temperature perturbations

Seafloor heat-flux measurements rely on the assumption that both long- and short-term bottom-water temperature variations are small; the volume of ocean bottom water is very large and the temperature of the source in polar regions is regulated by the formation of sea ice. Many early measurements were made with temperatures determined at only three depths over a span of a few meters, however. Good checks on the validity of this assumption were not possible until temperature observations began to be made in deep-sea boreholes and long records of bottom-water temperature were acquired (Hyndman et al., 1984; Davis et al., 2003). An ideal suite of observations that would allow errors associated with bottom-water temperature variations to be quantified throughout the world's oceans – one that is broadly distributed both geographically and with ocean depth – does not yet exist, but the available data show that gradients measured a few meters below the seafloor generally do permit accurate determinations of heat flux in large areas of the oceans where depths are greater than ~2,000 m. One example where errors are demonstrated to be small is illustrated in Figure 4, where closely colocated seafloor probe and borehole observations are compared. Significant bottom-water temperature variations are ruled out by the linearity of the plots of temperature versus cumulative thermal resistance, and by the agreement between the shallow probe and deep borehole determinations. This illustration also shows the importance of precise colocation when doing such a comparison, given the local spatial variability of heat flux as defined by neighboring probe measurements.

A more direct approach uses observations of bottom-water fluctuations. An example from a 5,000-m-deep site in the western Atlantic (Figure 5a) shows that in this area, oceanographic perturbations might have a modest influence on measured gradients. Estimated gradient perturbations at depths of less than 2–3 m below the seafloor range up to 10 mK m^{-1} (Figure 5b), that is, up to 20% of the geothermal gradient if the heat flux were 50 mW m^{-2}. A second example from a 2,600-m-deep site in the eastern Pacific shows smaller variability (Figure 5c), although perturbations estimated at a depth of 2 m could still result in a heat-flux determination error of up to 10%. Observations like these are clearly useful for guiding measurement strategy (e.g., depth of penetration) wherever heat flux is low and precise determinations are required.

Heat-flux signals from hydrothermal circulation

Hydrothermal circulation is a major source of error when determinations of deep-seated heat flux are sought, but it

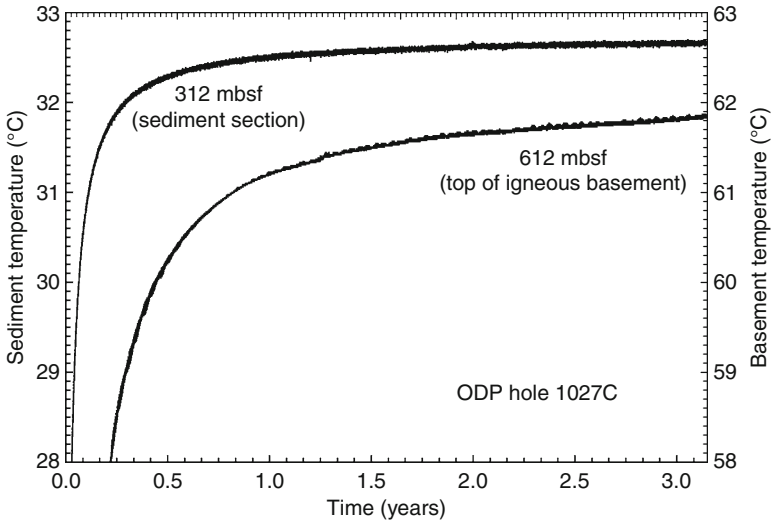

Heat Flow, Seafloor: Methods and Observations, Figure 3 Two records from a 10-thermistor cable suspended in a borehole that penetrates a c. 600-m-thick sediment layer and into the underlying uppermost igneous oceanic crust. The longer recovery time at the deeper level reflects the large volume of water that invaded the uncased and permeable igneous section during the 5 days between the time of drilling and when the hole was sealed and instrumented.

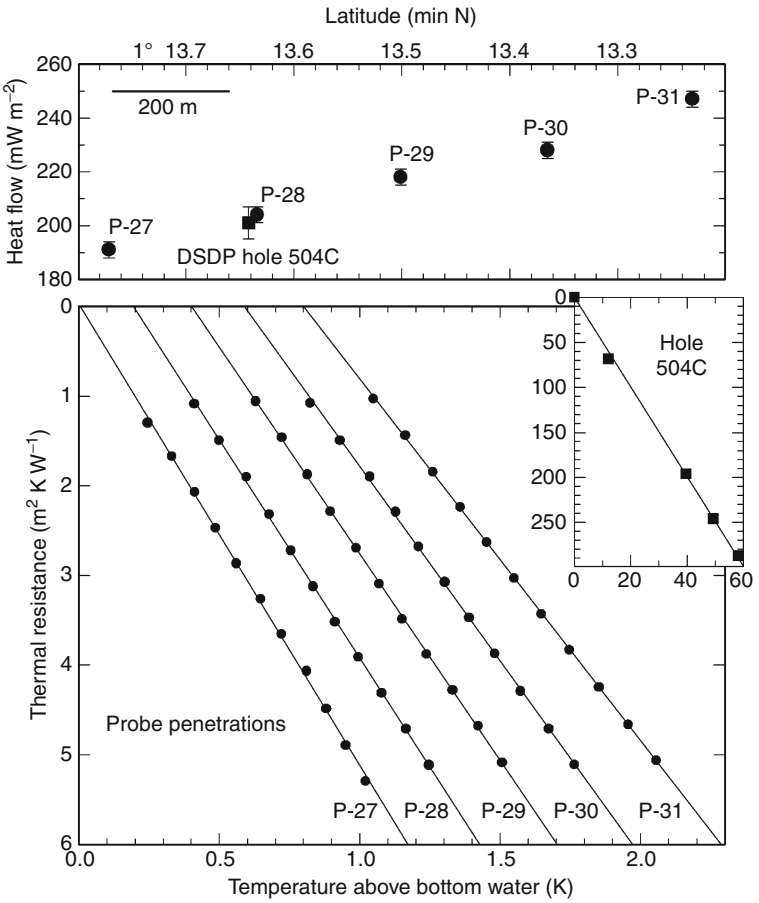

Heat Flow, Seafloor: Methods and Observations, Figure 4 Comparison of colocated seafloor probe and borehole heat-flux observations. Variations in probe measurements along the transect adjacent to the borehole site illustrate how carefully such comparisons must be done.

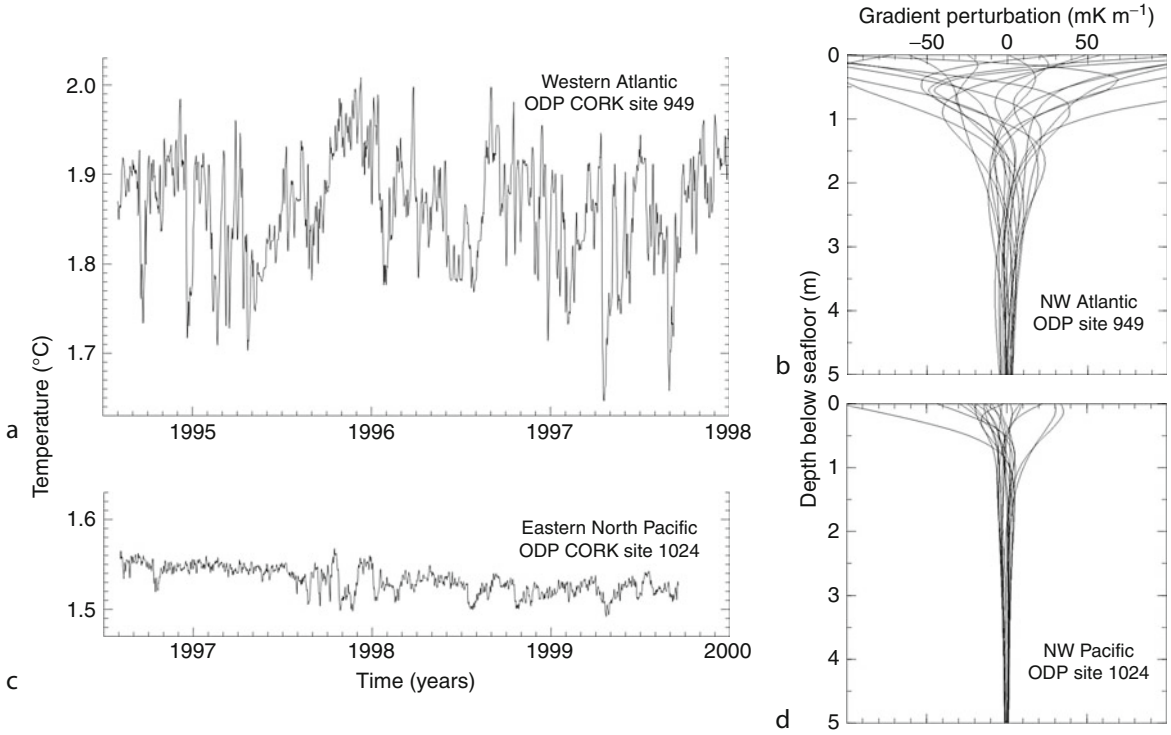

Heat Flow, Seafloor: Methods and Observations, Figure 5 Bottom-water temperature variations observed in the Atlantic (**a**) and Pacific Oceans (**c**), and estimated perturbations of the geothermal gradient as a function of depth (**b** and **d**) stemming from the variations, calculated at an evenly distributed suite of times during the temperature time series.

is also an important geological process. Hence it has been the focus of a large number of studies. Instructive examples of the influence of hydrothermal circulation are shown in Figure 6, where closely spaced measurements were made along transects striking perpendicular to basement structure. The first (Figure 6a) is in an area where sediment cover is continuous over a broad region spanning several tens of kilometers. Locally, heat flux varies inversely with sediment thickness. Such variations are common in areas of young seafloor, but can occur across relatively old seafloor as well (Embley et al., 1983; Von Herzen, 2004; Fisher and Von Herzen, 2005). They are the consequence of thermally efficient, local convection in permeable igneous rocks beneath low-permeability sediment cover. If the permeability of the igneous "basement" formation is high, vigorous convective flow maintains nearly constant temperatures at the sediment/basement interface despite variations in the thermal resistance of the overlying sediment layer. In this instance, the average seafloor heat flux is close to that expected from the underlying lithosphere, suggesting that from a thermal perspective, the circulation in the upper igneous crust is sealed in by the extensive sediment cover. The second transect (Figure 6b) crosses a sediment-covered area immediately adjacent to an area of outcropping igneous crust (where measurements are impossible). Local variations like those in Figure 6a are present, but even more apparent is a systematic variation of a larger scale, with heat flux increasing with distance from the area of basement outcrop, opposite to the expected trend of decreasing heat flux with increasing seafloor age. Temperatures estimated at the top of the igneous section increase systematically as well, suggesting that heat is transported laterally by fluid circulation and mixing in the sediment-sealed igneous crust. Heat exchange between the well-ventilated and sediment-sealed areas, indicated by the heat-flux deficit in this example, suggests a lateral heat-transfer scale of 20 km. Examples elsewhere suggest that the effects of advective heat loss may be felt laterally as far as 50–100 km (e.g., Fisher et al., 2003).

Ever since the early work of Lister (1972), the mere presence of local variability has been used as a diagnostic indicator of hydrothermal circulation in both young and old areas (e.g., Figure 6c), but with widely spaced observations, neither of the signals exemplified in Figure 6a and b could be resolved coherently; values were simply scattered and averages were often low. When systematic, detailed transects of observations began to be completed in context of colocated seismic data, the vigor of the convection could be inferred quantitatively from the nonconductive thermal regime (Fisher and Becker, 1995; Davis et al., 1997b), and the amount of heat lost

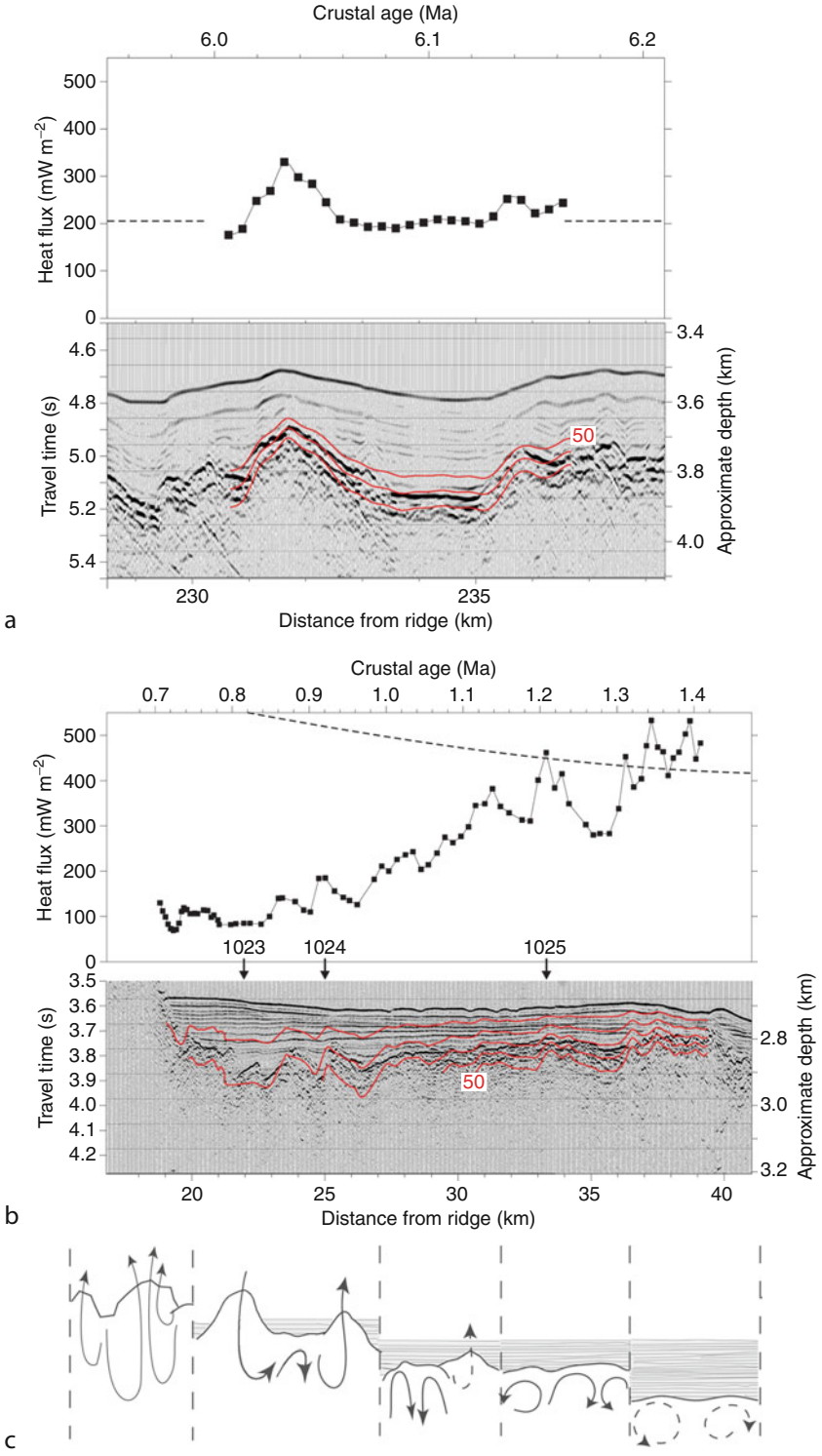

Heat Flow, Seafloor: Methods and Observations, Figure 6 Transects of heat flux on the flanks of the Costa Rica Rift (**a**) where an extensive sediment cover is present, and Juan de Fuca Ridge (**b**) striking away from an area of extensive basement at the left end of the figure. Both show the effects of hydrothermal circulation on conductive seafloor heat flux and on the crustal thermal regime. Heat flux estimated on the basis of the local lithosphere age (see text) is shown as the dashed lines. Temperatures estimated below the seafloor are shown at intervals of 10 °C. The cartoons in (**c**) show the influence of sediment burial on hydrothermal circulation and advective heat loss under a variety of burial states.

from the crust by fluid advection could be estimated with growing confidence (e.g., Anderson and Skilbeck, 1980; Stein and Stein, 1994; Harris and Chapman, 2004).

Two major lessons are learned from detailed observations like these for drawing conclusions about deep-seated heat flux. First, to ensure that observations do not suffer from the bias caused by convective ventilation, it must be demonstrated that there are no exposures of permeable rock at faults or volcanic edifices within distances of several tens of kilometers. Second, large numbers of closely spaced observations must be made, ideally colocated with seismic reflection data, so that the local variability can be understood and meaningfully averaged, and the locally relevant lateral transport scale can be assessed (e.g., Sclater et al., 1976; Davis et al., 1999).

Lessons learned about the way that the seawater interacts with the oceanic crust are far-reaching and continuously expanding. Estimates for the temperatures of circulation, the chemistry of the fluids, the volumetric rates of exchange between the crust and the ocean, and the consequent effects on crustal alteration and ocean chemistry have become reasonably well understood (e.g., Mottl and Wheat, 1994; Elderfield and Schultz, 1996). Studies of the actual distribution of crustal permeability, the percentage of rock affected by hydrothermal alteration, and the potential for chemosynthetic microbial populations are the focus of current investigations.

Dependence of heat flux on age and the global average

With the potentially large influence of hydrothermal circulation in mind, it is clear that a simple compilation of heat-flux data will provide a deceiving view of global heat loss. Except in old ocean basins, values are likely to be scattered and low relative to the heat loss expected from the underlying lithosphere. But by taking only those measurements that are sufficiently far from known permeable crustal outcrops and sufficiently numerous to provide a reliable local average, a subset of data can be gathered that provides a reliable determination of deep-seated heat flux. When considered in the context of lithospheric age, the results have been found to be consistent with both the characteristics of age-dependent seafloor subsidence and with simple lithospheric cooling theory (see *Lithosphere, Oceanic: Thermal Structure*). In young areas, heat flux is found to decline linearly with the inverse square root of age, following the simple relationship $Q = \mathrm{C}\, t^{-1/2}$ (where Q is heat flux in $\mathrm{mW\,m^{-2}}$, t is age in Ma, and C is a constant estimated between 475 and 510; Lister, 1977; Harris and Chapman, 2004). High-quality observations in older regions ($>$100 Ma) are generally uniform, in the range of 45–50 $\mathrm{mW\,m^{-2}}$ (Lister et al., 1990), suggesting that the thermal structure of the lithosphere may become stabilized in a state regulated either by the convectively supplied heat flux from the underlying asthenosphere, or by the combination of a compositionally established lithospheric thickness and the relatively uniform temperature of the vigorously convecting asthenosphere.

With the relationship between heat flux and age thus defined, the problems of the unknown bias and large scatter in young areas and the sparse distribution of measurements in large portions of the oceans can be overcome. A reliable estimate for the total heat flow through the floor of the ocean can be had by using the area/age relationship for the oceans defined by seafloor magnetic anomalies (e.g., Parsons, 1982; Wei and Sandwell, 2006), along with a robust heat-flux/age relationship. Several such estimates have been made (e.g., Williams and Von Herzen, 1974; Sclater et al., 1980; see summary in Jaupart et al., 2007), and all fall in a relatively narrow range centered around 32 TW (with contributions from marginal seas and hotspot swells included). This yields an average seafloor flux of roughly 107 $\mathrm{mW\,m^{-2}}$, a number that has little physical significance, but is considerably greater than that estimated in the early days of marine heat flow, and greater than the average though continents (c. 67 $\mathrm{mW\,m^{-2}}$), particularly when the latter is adjusted for the contribution of continental crustal radiogenic heat (c. 33 $\mathrm{mW\,m^{-2}}$).

With the total heat flow thus constrained, the heat lost advectively by ventilated circulation can be estimated from the difference between this and the age-binned average of unfiltered observations. Such estimates of this "heat deficit" fall in the neighborhood of 10 TW (Stein and Stein, 1994; Harris and Chapman, 2004). Most of this deficit occurs in seafloor less than 8–10 Ma in age, and it becomes insignificant on average by an age of 65 Ma. The actual age at which advective loss becomes insignificant is locally variable, depending primarily on the continuity of accumulating sediments that bury the igneous crust (Anderson and Skilbeck, 1980; Harris and Chapman, 2004), and the associated increase in spacing between basement outcrops that are essential for hydrothermal recharge and discharge on older ridge flanks (Fisher and Wheat, 2010).

The signature of subduction

Marine heat flux is used extensively to constrain deep thermal structure in studies of continental margins and marginal basins. A transect crossing the forearc prism of the Cascadia subduction zone illustrates one such application (Figure 7). This transect begins with standard gravity-driven probe measurements over the incoming plate and outermost accretionary prism, where bottom-water temperature variability is small. Where the seafloor is shallower than 1,500–2,000 m, other measurement techniques are used, including borehole measurements and estimates made using the depth to a bottom-simulating seismic reflector (BSR), which marks the limit of methane-hydrate stability. This reflector defines a unique set of pressure-temperature conditions, and with constraints on seismic velocity and thermal conductivity of the section above the BSR, the thermal gradient and heat flux can be estimated. Alternatively, a small set of seafloor

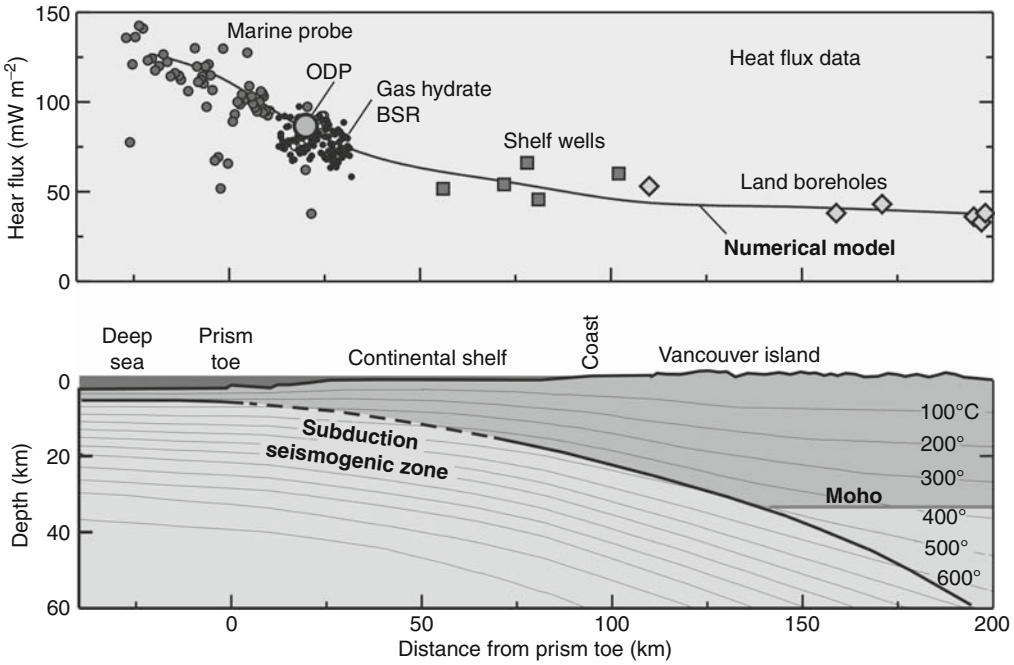

Heat Flow, Seafloor: Methods and Observations, Figure 7 Structural and heat-flux transect across the Cascadia subduction forearc, with temperatures estimated from a numerical model for underthrusting and sediment thickening, constrained by the heat-flux data (following compilation of Hyndman and Wang, 1993).

heat-flux measurements can be used as a "calibration." In either case, the travel-time depth to BSRs can serve as a widespread proxy for thermal data (e.g., Yamano et al., 1982). This technique is valuable where bottom-water temperature variability is too large to permit accurate heat-flux determinations with shallow probes, where sediments are too hard to allow probe penetration, or where there are few conventional measurements. Observations like these allow the thermal structure to be inferred deep within subduction zones, providing a critical constraint on the rheology of the rocks and the potential for seismogenic slip along the subduction thrust interface. In the example shown (Figure 7), the seafloor heat flux is variable locally, but regional values and trends are consistent with the expected thermal state of the thickly sedimented subducting plate.

In another study of the subducting Cocos Plate seaward of the Middle America Trench, variations in the thermal state of the plate are strongly influenced by regional differences in hydrothermal heat loss, and these correlate with differences in seismic processes occurring at depth (Newman et al., 2002; Fisher et al., 2003). One part of the plate is extensively cooled by hydrothermal circulation before the Cocos Plate is subducted, and earthquakes observed within the subduction wedge in this area are relatively deep (>20 km). Earthquakes tend to be shallower (<20 km) along an adjacent segment of the subduction zone, where there is no evidence for regional advective heat extraction. One explanation for the different earthquake depths is that cooling of part of the Cocos Plate slows dewatering and the transition of smectite to illite in subducting sediments (Spinelli and Saffer, 2004). Illite-rich sediments are more likely to undergo brittle deformation at depth, so the delay in heating associated with hydrothermal circulation in the crust prior to subduction causes a landward shift of the locked region where earthquakes are most likely to occur.

Summary

Seafloor heat flux can be measured with high accuracy in most deep-ocean settings with gravity-driven probes that penetrate a few meters into seafloor sediment. Improvements in heat-flux measurement technology, improvements in navigation, and integration with swath bathymetric, seismic, and other data that provide geological context for heat-flux measurements have greatly advanced our understanding of many global, regional, and local heat flow processes. Comparison of seafloor and borehole data has demonstrated that measurements made with short probes are accurate, provided that bottom-water temperature variations are relatively small. Compilations of global heat-flux data show that heat flux tends to vary systematically with seafloor age, following a $t^{-1/2}$ relation, at least until seafloor age exceeds 100 Ma, after which heat flux tends to become relatively constant. Determining the deep-seated lithospheric heat flux requires quantification of the potentially large influence of hydrothermal circulation in the permeable igneous rocks of the upper oceanic crust. This is best accomplished

through closely spaced transects of heat-flux measurements colocated with seismic reflection profiles that constrain the hydrologic structure, and regional maps that allow identification of basement outcrops. This approach has been applied in numerous settings, providing valuable constraints on the flow of water within the oceanic crust, the exchange of water, heat, and solutes between the crust and the oceans, the formation of hydrothermal mineral deposits, the accumulation of gas hydrates, and the development and maintenance of a subseafloor microbial biosphere. Individual heat-flux measurements and transects of measurements can be extended across broad regions using the depth to bottom-simulating seismic reflectors. These and other applications were never imagined by those who developed the original techniques for acquisition of seafloor heat-flux data 6 decades ago, but they illustrate how acquiring this kind of data has remained valuable for multidisciplinary studies of thermal, hydrogeologic, tectonic, and microbiological conditions and processes within the lithosphere.

Bibliography

Anderson, R. N., and Skilbeck, J. N., 1980. Oceanic heat flow. In Emiliani, C. (ed.), *The Sea*. New York: Wiley Interscience, Vol. 7, pp. 489–523.

Bullard, E. C., 1954. The flow of heat through the floor of the Atlantic Ocean. *Proceedings of the Royal Society A*, **222**, 408–429.

Davis, E. E., Wang, K., He, J., Chapman, D. S., Villinger, H., and Rosenberger, A., 1997a. An unequivocal case for high Nusselt number hydrothermal convection in sediment-buried igneous oceanic crust. *Earth and Planetary Science Letters*, **146**, 137–150.

Davis, E. E., 1988. Oceanic heat-flow density. In Haenel, R., Rybach, L., and Stegena, L. (eds.), *Handbook of Terrestrial Heat-Flow Density Determination*. Dordrecht: Kluwer, pp. 223–260.

Davis, E. E., Becker, K., Pettigrew, T., and Carson, B., 1992. CORK: a hydrologic seal and downhole observatory for deep-sea boreholes. *Proceedings ODP, Init. Repts.* 139, pp 45–53.

Davis, E. E., Villinger, H., Macdonald, R. D., Meldrum, R. D. J., and Grigel, J., 1997b. A robust rapid-response probe for measuring bottom-hole temperatures in deep-ocean boreholes. *Marine Geophysical Researches*, **19**, 267–281.

Davis, E. E., Chapman, D. S., Wang, K., Villinger, H., Fisher, A. T., Robinson, S. W., Grigel, J., Pribnow, D., Stein, J. S., and Becker, K., 1999. Regional heat flow variations on the sedimented Juan de Fuca Ridge eastern flank: constraints on lithospheric cooling and lateral hydrothermal heat transport. *Journal of Geophysical Research*, **104**, 17675–17688.

Davis, E. E., Wang, K., Becker, K., Thomson, R. E., and Yashayaev, I., 2003. Deep-ocean temperature variations and implications for errors in seafloor heat flow determinations. *Journal of Geophysical Research*, **108**, 2034, doi:10.1029/2001JB001695.

Elderfield, H., and Schultz, A., 1996. Mid-ocean ridge hydrothermal fluxes and the chemical composition of the ocean. *Annual Review of Earth and Planetnery Sciences*, **24**, 191–224.

Embley, R. W., Hobart, M. A., Anderson, R. N., and Abbott, D., 1983. Anomalous heat flow in the northwest Atlantic: a case for continued hydrothermal circulation in 80-M.y. crust. *Journal of Geophysical Research*, **88**, 1,067–1,074.

Fisher, A. T., and Becker, K., 1995. The correlation between heat flow and basement relief: observational and numerical examples and implications for upper crustal permeability. *Journal of Geophysical Research*, **100**, 12,641–12,657.

Fisher, A. T., and Von Herzen, R. P., 2005. Models of hydrothermal circulation within 106 Ma seafloor: Constraints on the vigor of fluid circulation and crustal properties below the Madeira Abyssal Plain, *Geochemistry, Geophysics, Geosystems*, **6**, 17 pp doi:10.1029/2005GC001013.

Fisher, A. T., and Wheat, C. G., 2010. Seamounts as conduits for massive fluid, heat and solute fluxes on ridge flanks. *Oceanography*, **23**(1), 74–87.

Fisher, A. T., Stein, C. A., Harris, R. N., Wang, K., Silver, E. A., Pfender, M., Hutnak, M. C., Cherkaoui, A., Bodzin, R., and Villinger, H., 2003. Abrupt thermal transition reveals hydrothermal boundary and role of seamounts within the Cocos plate. *Geophysical Research Letters*, **30**(11), 1550, doi:10.1029/2002GL016766.

Harris, R. N., and Chapman, D. S., 2004. Deep-seated oceanic heat flux, heat deficits, and hydrothermal circulation. In Davis, E. E., and Elderfield, H. (eds.), *Hydrogeology of the Oceanic Lithosphere*. New York: Cambridge University Press, pp. 311–336.

Horai, K., and Von Herzen, R. P., 1985. Measurement of heat flow on Leg 86 of the Deep Sea Drilling Project, in *Init. Repts., DSDP* 86, pp. 759–777.

Hyndman, R. D., 1984. Review of Deep Sea Drilling Project geothermal measurements through Leg 71. *Init. Repts. DSDP* 78B, pp. 813–823.

Hyndman, R. D., Davis, E. E., and Wright, J. A., 1979. The measurement of marine geothermal heat flow by a multipenetration probe with digital acoustic telemetry and in situ thermal conductivity. *Marine Geophysical Researches*, **4**, 181–205.

Hyndman, R. D., and Wang, K., 1993. Thermal constraints on the zone of major thrust earthquake failure: the Cascadia subduction zone. *Journal of Geophysical Research*, **98**, 2039–2060.

Jaupart, C., Labrosse, S., and Mareschal, J.-C., 2007. Temperatures, heat, and energy in the mantle of the Earth. In Bercovici, D. (ed.), *Treatise on Geophysics.* Oxford: Elsevier Vol. 7, pp 253–303.

Lee, W. H. K., and Uyeda, S., 1965. Review of heat flow data in Lee, W. H. K. (ed.), *Terrestrial Heat Flow, Geophysical Monograph 8*, Washington: American Geophysical Union, pp. 87–190.

Lister, C. R. B., 1972. On the thermal balance of a mid-ocean ridge. *Geophysical Journal International*, **26**, 515–535.

Lister, C. R. B., 1977. Estimators for heat flow and deep rock properties based on boundary layer theory, Tectonophysics, **41**, 157–171.

Lister, C. R. B., 1979. The pulse-probe method of conductivity measurement. *Geophysical Journal of Royal Astronomical Society*, **57**, 451–461.

Lister, C. R. B., Sclater, J. G., Davis, E. E., Villinger, H., and Nagihara, S., 1990. Heat flow maintained in ocean basins of great age: investigations in the north-equatorial west Pacific. *Geophysical Journal International*, **102**, 603–630.

Mottl, M. J., and Wheat, C. G., 1994. Hydrothermal circulation through mid-ocean ridge flanks: fluxes of heat and magnesium. *Geochimica et Cosmochimica Acta*, **58**, 2,225–2,237.

Newman, A. V., Schwartz, S. Y., Gonzalez, V., DeShon, H. R., Protti, J. M., and Dorman, L. M., 2002. Along-strike variability in the seismogenic zone below Nicoya Peninsula, Costa Rica. *Geophysical Research Letters*, **29**, 1–4, doi:10.1029/2002GL015409.

Parsons, B., 1982. Causes and consequences of the relation between area and age of the ocean floor. *Journal of Geophysical Research*, **87**, 289–303.

Petterson, H., 1949. Exploring the bed of the ocean. *Nature*, **4168**, 468–470.

Revelle, R. R., and Maxwell, A. E., 1952. Heat flow through the floor of the eastern North Pacific Ocean. *Nature*, **170**, 199–202.

Sclater, J. G., Crowe, J., and Anderson, R. N., 1976. On the reliability of ocean heat flow averages. *Journal of Geophysical Research*, **81**, 2,997–3,006.
Sclater, J. G., Jaupart, C., and Galson, D., 1980. The heat flow through oceanic and continental crust and the heat loss of the earth. *Reviews of Geophysics*, **18**, 269–311.
Spinelli, G. A., and Saffer, D., 2004. Along-strike variations in underthrust sediment dewatering on the Nicoya margin, Costa Rica related to the updip limit of seismicity. *Geophysical Research Letters*, **31**, 1–5, doi:10.1029/2003GL018863.
Stein, C. A., and Stein, S., 1994. Constraints on hydrothermal heat flux through the oceanic lithosphere from global heat flow. *Journal of Geophysical Research*, **99**, 3,081–3,095.
Uyeda, S., and Horai, K. 1980. Heat flow measurements on Deep Sea Drilling Project Leg 60, in *Init. Repts., DSDP* 60, pp 789–800, Washington, U. S. Govt. Printing Office.
Von Herzen, R. P., and Uyeda, S., 1963. Heat flow through the eastern Pacific Ocean floor. *Journal of Geophysical Research*, **68**, 4,219–4,250.
Villinger, H., and Davis, E. E., 1987. A new reduction algorithm for marine heat flow measurements. *Journal of Geophysical Research*, **92**, 12,846–12,856.
Von Herzen, R. P., 2004. Geothermal evidence for continuing hydrothermal circulation in older (> 60 M.y.) ocean crust. In Davis, E. E., and Elderfield, H. (eds.), *Hydrogeology of the Oceanic Lithosphere*. Cambridge: Cambridge University Press, pp. 414–447.
Wei, M., and Sandwell, D., 2006. Estimates of heat flow from Cenozoic seafloor using global depth and age data. *Tectonophysics*, **417**, 325–335.
Williams, D. L., and Von Herzen, R. P., 1974. Heat loss from the earth: new estimate. *Geology*, **2**, 327–330.
Williams, D. L., Von Herzen, R. P., Sclater, J. G., and Anderson, R. N., 1974. The Galapagos spreading center: Lithospheric cooling and hydrothermal circulation. *Geophysical Journal of Royal Astronomical Society*, **38**, 587–608.
Wright, J. A., and Louden, K. E., 1989. *Handbook of Seafloor Heat Flow.* Boca Raton: CRC Press. 498 pp.
Yamano, M., Uyeda, S., Aoki, Y., and Shipley, T. H., 1982. Estimates of heat flow derived from gas hydrates. *Geology*, **10**, 339–343.

Cross-references

Heat Flow Measurements, Continental
Heat Flow, Continental
Lithosphere, Continental: Thermal Structure